Simulation and optimization of pilot reverse osmosis desalination plant powered by photovoltaic solar energy

A. Lilane[a,*], D. Saifaoui[a], Y. Aroussy[a], M. Chouiekh[a], M.A. Sharaf Eldean[b], A. Mabrouk[c]

[a]Laboratory of Renewable Energy and Dynamic Systems, Faculty of Sciences Aîn Chock, Hassan II University of Casablanca, El-Jadida road Km9-BP 5366 Maarif Casablanca-Morocco, Mobile No. +212(0)626-144-316;
emails: amine.lilane-etu@etu.univh2c.ma/m.amine.lilane@gmail.com (A. Lilane), ddsaifaoui@gmail.com (D. Saifaoui),
aroussy110@gmail.com (Y. Aroussy), chouiekh.mohamed@gmail.com (M. Chouiekh)
[b]Department of Mechanical Engineering, Faculty of Engineering, Suez University, Egypt,
email: mohammed.eldeen@suezuniv.edu.eg
[c]Qatar Environment and Energy Research Institute, Hamad Bin Khalifa University, Qatar Foundation, Doha,
Qatar, email: aaboukhlewa@hbku.edu.qa

ABSTRACT

Solar photovoltaic (PV) can easily power the electrical membrane desalination processes at low specific power consumption (SPC), kWh/m³. Direct contact with the desalination pump systems is considered as a remarkable advantage for such techniques. In this work, solar PV with/without battery bank is connected to the reverse osmosis (RO) desalination system for a production rate of 1–10 m³/d. The system is aiming to produce a freshwater from brackish water sources. MATLAB/Simulink toolbox is used to simulate the real system under different operating conditions. In real time simulation is presented to measure the performance system during the day. Genetic algorithm is also used to optimize the system performance under different operating conditions. Results reveal that, increasing the solar radiation would increase the production system rate. The optimum system SPC is recorded between 2.5 and 4.5 kWh/m³. Meanwhile, the optimum recovery ratio for the RO is recorded between 15% and 19.5%.

Keywords: Solar energy; Photovoltaic; Reverse osmosis; Solar desalination; Genetic algorithm; Brackish water; Desalination

1. Introduction

There is a serious shortage of drinking water in some countries in the world, especially in the Middle East region and North Africa (MENA), including Morocco. According to the World Resources Institute (WRI) reported rate, more than a third of the world's population currently lives in areas where the amount of existing fresh water does not meet their needs [1]. Therefore, the desalination of seawater (SW) or brackish water (BW), is a process which makes it possible to obtain fresh (potable) water via several membrane, and/or thermal techniques. Desalination can be put in place against the challenges associated with water scarcity to meet and satisfy the needs of the population growth with a huge world production capacity [2,3]. Thanks to thousands of desalination plants around the world (more than 15 900 desalination plants operated in 2018), this production is still developing quite remarkably [4]. However, water covers almost three quarters of the planet's surface, about 97.5% of the earth's water is salt from the oceans and only 2.5% of fresh water from groundwater, lakes and rivers, provide most of human and animal

* Corresponding author.

needs. Tackling the problem of water scarcity involves more efficient and economical means of desalinating seawater or brackish water [5].

Drinking water production by using the desalination processes especially reverse osmosis (RO) because it is the most widely used technique (Fig. 1b) [6]. However it faces a high electricity consumption. At the same time, energy covers 60% of production costs in the thermal distillation technique, and 44% in RO membrane process [7]. High electricity consumption affects the environmental side and more importantly the production cost [8]. The consumption varies between 3.7 and 5.3 kWh/m^3 depending on the nature of water to be desalinated and the production quality [9]. In this sense, the economics of water desalination play an important factor on the industrial scale. Several criteria influence this factor, such as the quality of the intake and production water, the capital cost of the production plant, the source and the cost of the energy used, the costs of upkeep and maintenance and the financing interest rate [10]. Therefore, discovering and developing new energy sources rather than conventional sources like renewable energies to power plants and desalination stations, are very important. They can be considered as an alternative production of drinking water. Equally, they are very essential to limit this problem which remains one of the major weaknesses of the whole system despite more advanced and technological techniques, economic and industrial development [11]. These sources represent several advantages: availability throughout the year, free and inexhaustible energy, etc. In fact, the major challenge of desalination by renewable energies is that these techniques generally work under conditions where the operating energy is practically stable, and it is a permanent regime, but renewable energy sources are generally non-stationary, they depend on several factors. For this reason, the production of energy via a renewable source requires adjustments for a continuous supply; moreover, desalination technologies can adapt to variable operations [12]. The main aim of this work is to model, simulate, and examine the performance of the real solar photovoltaic (PV)/RO freshwater production system. It is quite important to enhance the performance of the system under different operating conditions. The system aimed to desalinate a brackish water source. For that purpose, the following pinpoints can be withdrawn as follows:

- Survey about the recent activity related to solar/renewable desalination regarding RO process.
- Demonstrate the proposed system and the supporting units.
- Modelling and simulation technique is presented.
- Mathematical and genetic algorithm (GA) models are presented.
- Real time simulation is presented based on the optimized results from the GA model.

2. Desalination and renewable energy

Throughout the world, solar energy is the most abundant form of renewable energy, and the most used in the desalination industry (Fig. 1a) [13], it has several advantages as we have briefly indicated before. Some statistical studies show that solar energy produced from 1% of arid or semi-arid areas could be sufficient to meet the energy demand of the whole world [14]. Accordingly, many regions of the Middle East and North Africa receive a very important daily irradiation frequented throughout the year; this irradiation varies between 4.5 to 7 kWh/m^2 per solar noon (Fig. 2a). These regions are also characterized by a very significant annual electrical potential (Solar photovoltaic), it varies between 5.2 to 6 kWh/kWh$_p$ (Fig. 2b) [15]. Morocco is one of these regions rich of brackish and seawater, but suffers from a remarkable lack of fresh water, especially in the Saharan, and the southern regions. In this sense, desalination seawater or brackish water based on solar energy is a proactive policy in the field of development and enhancement of water resources. It is considered as a very effective solution. In addition, it will become a reliable alternative against drought not only for Morocco: but also for many regions around the world (Fig. 2c) [16,17]. In the last few years, the desalination industry recognizes remarkable progress all over the world; it has been evolved in a speed and efficient manner through exploited in water
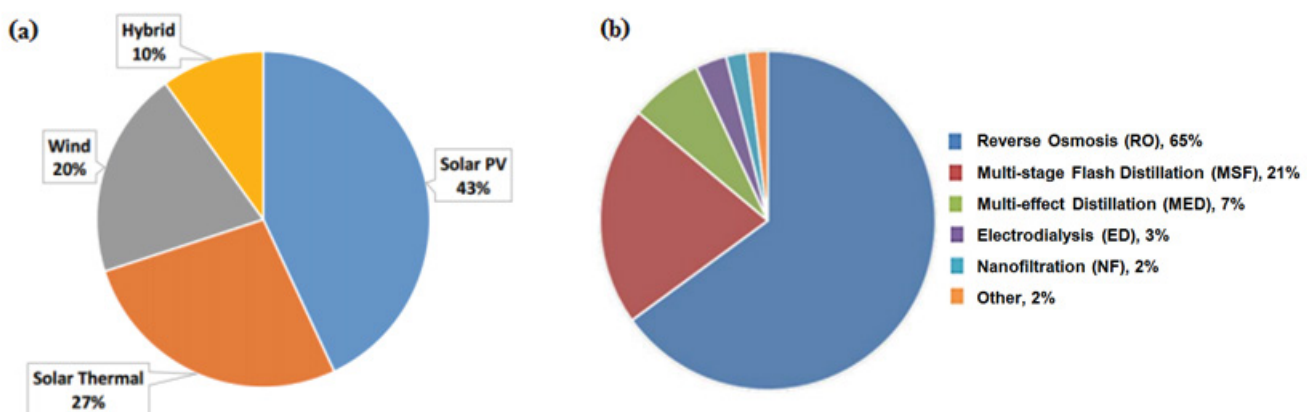

Fig. 1. (a) Exploitation rate of renewable energies for desalination [13]. (b) Usage and exploitation rate of desalination techniques worldwide [6].
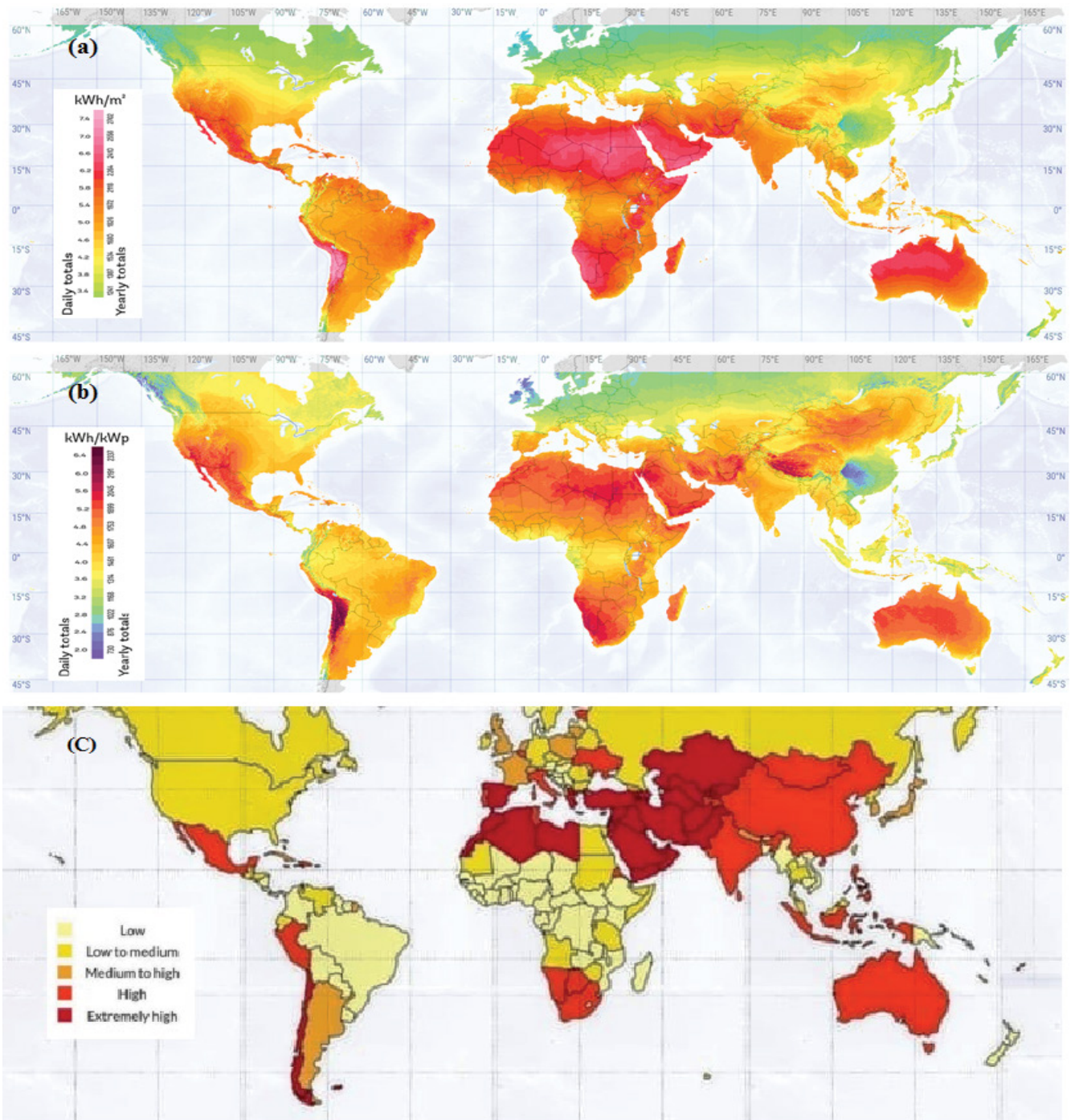
Fig. 2. (a) Long-term average of photovoltaic power potential (PVOUT). (b) Long-term average of global horizontal irradiation (GHI) [15]. (c) Water stress in the world.

treatment strategies. In effect, the exploitation of renewable energy in the desalination industry has an essential effect, especially on the quality-price ratio of the water produced, the exploitation of renewable energy resources reduces the energy cost of desalination plants, the thing that will reduce the overall cost of desalinated water. Despite this favorable combination of these sectors, the exploitation of renewable resources is still limited. It requires finding relevant solutions to develop these sectors. In this context, renewable energies and desalination researchers are developing several optimization methods and algorithms which aim to increase the functional and productive performance of this industry. Table 1 presents all the research work of recent years (from 2000 to 2021), which shows perfectly well that renewable desalination sector still needs improvements, and that is the objective of this work. Based on Table 1 and Fig. 2, it would become remarkably quite important to combine between solar PV and RO for freshwater production.

3. System description

This paper presents a prototype of a small brackish water reverse osmosis (BWRO) desalination unit which has been designed to adapt its consumption continuously to non-variable power supply. The RO/EV pilot system includes a reverse osmosis membrane (F2), brand DOW FILMETEC FT-30 (Table 2), two tanks; one for supply (D1) and the other for receiving the produced water (D2), an IP 55 electrical panel, and a synoptic of the entire desalination plant and other measuring instruments such as flow meters, barometers, etc. (Fig. 3). The studied desalination system comprises an asynchronous alternating current machine of TECHTOP brand, type MS2 100L4 of 2.2 kW (Table 3), coupled to a piston pump which supplies the small capacity reverse osmosis desalination unit. Carrying the energy produced by a single solar cell is not sufficient to power the desalination system; thus, it is compulsory to gather the cells in series and to have the desired power in parallel to return the system to normal steady-state operation.

A dimensional study that has been executed is based on a brand photovoltaic solar panel: Amerisolar, Model AS-6P30 (Table 3) made to ensure the total number of GPVs necessary to couple it by photovoltaic energy, considering that the appropriate solar field for GPV desalination system must be composed of 14 PV panels connecting in series and in parallel generating a nominal peak power 4.00 kW_p (at noon) connected to a DC bus via a DC-DC converter to push the solar field to produce their maximum power during the nominal operation of the desalination system. The conversion of DC bus to another AC is done by a DC-AC converter (3 ~) to supply the machine part of the reverse osmosis unit (Fig. 3a). Because of that the system becomes autonomous (Fig. 3b), the intermittence of the energy source used in this system requires storage of electrical energy in the batteries, as listed in Table 3; (Battery Hoppecke Sun power VL 2-1700). That would be important to ensure the normal functioning of the system in case the solar photovoltaic system does not produce any energy (by night for example). In such systems the batteries are the intermediate between DC-DC and DC-AC converters; this location

has several advantages: the power produced, and the nominal voltage of the system are practically stable and they ensure a very high starting current during the operation, etc.

4. Mathematical and GA optimization models

It is quite important for any modelling and simulation system to withdraw and present the mathematical model and the modelling technique that has been adopted. For that purpose, MATLAB/Simulink model has been built to simulate the real system. The model includes the blocks which represent each unit. Behind each block (double click), the code equations that represent this unit is performed by modelling each unit, it will become easier to connect all the units for the simulation results. Because of the existence of the real system, the model type is considered as a performance type not a design type. Concerning performance type, the flow rate, solar radiation, areas, sizes, ambient temperature, etc., are kept known parameters. The calculation parameters are productivity, salinity profiles, salt rejection percentage, brine, power, efficiency, etc. Fig. 4 shows the system units model under MATLAB/Simulink browser.

4.1. Photovoltaic generator mathematical model

The low efficiency of the conversion of photon energy to electric energy is one of the two major problems of solar PV systems which limits this technology, intermittence is another major problem which has a continuous change in quantity of electrical energy generated by the PV solar field due to the variations of metrological conditions (duration and period of irradiation, solar masks, etc.) [38,39]. In addition to, the Current-Voltage (I-V) characteristic of a PV generator is non-linear; it varies with the variation in irradiation and temperature [40]. The model of the solar cell used in this work is a simplified equivalent circuit. It is constituted of a single diode for cell polarization phenomena and two resistors (series and shunt) for the losses [41]. Therefore, it can be called "one-diode model". This model is used by manufacturers through by giving the technical characteristics of their solar cells [42,43]. For the PV system [44,45], it is quite important to address the system performance by the main specifications of the PV. Such specifications can be concluded in some parameters like short circuit current, open-circuit voltage, photon current, saturation current, maximum current and voltage. For short circuit current, I_{scr}, Amp, the following correlation can execute it based on open-circuit voltage, V_{oc}, V, and solar radiation, I_s, W/m².

$$I_{scr} = 0.1682 + 0.0008328 \times I_s - 0.003672 \times V_{oc} + 3.053e$$
$$- 06 \times I_s \times V_{oc} + 1.562e - 05 \times V_{oc}^2 - 6.45e - 09 \times I_s$$
$$\times V_{oc}^2 - 1.717e - 08 \times V_{oc}^3 \tag{1}$$

For photon current, it can be calculated based on I_{scr}, Å, short-circuit coefficient (=0.0017, Å/°C), and ambient temperature, T_a, °C.

$$I_{ph} = \left(I_{scr} + KI \times \left(T_a + 273 - 298 \right) \right) \times \frac{I_s}{1,000} \tag{2}$$

Table 1
Comparison of the optimization methods of the desalination systems from 2000 to 2021

S. No.	Year	Configuration	Type of RO membrane	S (ppm)	Capacity (m³/d)	SPC (kWh/m³)	Wco ($/m³)	Description of the used method	References
1	2000	PV-Batt-BWRO	SWRO	6,000	5.00	0.06	6.52	The desalination of brackish water in the region studied was experimentally realized without optimization of the system.	[18]
2	2001	PV-Batt-SWRO	SWRO	–	5.00	15	–	The objective of this study is to optimize the operating mode of the desalination system by focusing on the operational strategy, as well as the batteries energy storage regulation, in order to increase their lifetime, and ensure the right functioning of the system with the minimum equipment, this concern: static, flexible and dynamic regulations strategies.	[19]
3	2002	PV-SWRO	SWRO	40,000	3.90	–	2.18	The objective of this study is to maximize the overall efficiency of the system and the rate of water harvesting by using a solar field maximum power point (MPPT) tracking algorithm.	[20]
4	2004	Wind-SWRO	SWRO	45,094	18.9	4.2	–	The objective of this study is to maximize water recovery rate of the membrane studied, by using a programmable controller to look for an optimal operating pressure system and increase the flow production.	[21]
5	2008	PV-SWRO	SWRO	35,000	0.82	6.00	8.47	The desalination of seawater in the region studied was experimentally realized without the optimization of the system.	[22]
6	2008	PV-Batt-SWRO	SWRO	–	0.35	4.60	7.8	This experimental study was realized in order to compare the different operation modes of the desalination system; the results show perfectly that the direct coupling PV-SWRO without storage is the optimal mode, despite the amount of water produced is reduced up to 41.67%.	[23]
7	2008	PV-Batt-SWRO	BWRO	32,900	5	2.4	1.2	This study aims to optimize the productive mode of the installation, is about an optimization algorithm which will make it possible to seek an optimal configuration system and will increase the water recovery rate and to reduce the cost of production.	[24]

Table 1 Continued

S. No.	Year	Configuration	Type of RO membrane	S (ppm)	Capacity (m³/d)	SPC (kWh/m³)	Wco ($/m³)	Description of the used method	References
8	2010	PV-Wind-SWRO-WT	SWRO	–	–	3	2.44	The purpose of this study is to reduce the cost of the freshwater produced, by optimizing the operating mode of all the desalination system using a digital computer program.	[25]
9	2012	Grid-SWRO	SWRO	40,000	2,000	2.97	0.1	The objective of this work is to minimize the energy consumption of the desalination plant by integrating the energy recovery technique based on the Pelton Turbine using the DEEP-3.2 software.	[26]
10	2013	PV-Wind-Batt-SWRO	SWRO	–	5.00	5.0	3.81	Reducing the electrical power supply losses and optimize the dimensions of the hybrid desalination system and reduce the cost of a cubic meter of the water produced is the main objective of this study.	[27]
11	2013	PV-Wind-Batt-SWRO	SWRO	–	15.00	0.038	2.62	The authors manage to minimize the cost of water produced from the hybrid desalination system, using the genetic algorithm as a method of optimizing the operation and structure of the system.	[28]
12	2015	PV-SWRO	SWRO	48,761	200	6.99	0.82	The aim of this work is to make a feasibility study of the optimization amount of subsidized freshwater in Abu Dhabi City, by modeling a desalination plant using ROSA software, that will reduce the subsidy bill up to 43.2%.	[29]
13	2016	PV-SWRO-WT	SWRO	–	10	1.10	3.74	The optimization method used in this work is a multi-objective optimization algorithm resulting from a combination between the numerical technique of the Freshwater Pinch Analysis (FWaPA) and the genetic algorithm to ensure a good exploitation of the PV-RO-WT system by minimizing the outsourcing of freshwater, installation equipment, etc.	[30]
14	2016	PV-Batt-BWRO	SWRO	2,000	5.1	1.1	–	The major aim of this work is to compare the different reverse osmosis membrane types, in order to choose the suitable model, and optimize the batteries autonomy duration, by cooling their temperature to an optimal operating value using cooling fans.	[31]

| No.	Year	System	Type					Description	Ref.
15	2016	PV-Batt-BWRO	BWRO/NF	3,632	1.58	1.6	–	The aim of this work is choosing the appropriate membrane filtration for the system, by comparing the different types of reverse osmosis and nanofiltration membranes, the choice of the NF90 member was made due to their high performance of quality/quantity of water produced.	[32]
16	2018	PV-Wind-SWRO-WT	SWRO	–	10	4	–	In this research the main idea is that the authors are succeeded in developing a new hybrid optimization algorithm suitable for the different configurations of the desalination system studied to increase their functional and productive preferences, and choose the most efficient configuration.	[33]
17	2019	PV-Wind-Batt-SWRO	SWRO	–	3.63	8.93	0.25	The energy source of the desalination unit in this study is managed by the artificial neural network (ANN) method, in order to optimize the electrical production under climatic variability and intermittence, and also the unstable amount of water according to demand.	[34]
18	2020	PV-SWRO	SWRO	3,500	10.00	2.80	1.65	The optimization method used in this study is the optimization of the system supply pressure in order to increase it and reduce the number of membrane elements of the installation as well as the cost of water produced, this optimization was realized on the basis of determining the average values of the technical input parameters of the production system with the aim of finding an optimal average operating pressure.	[35]
19	2021	PV-Batt-SWRO	SWRO	–	100.00	4.50	2.69	Developing the Python-Spyder software, basing on algorithms to optimize the tilt angle of PV modules, to improve the productive capacity of the desalination system and the cost of water.	[36]
20	2021	Microgrid-RE-SWRO	SWRO	–	26.31	1.32	–	This study was achieved by using desalination Plant software, to minimize the cost of desalination that optimize and manage the electrical flow generated by the power supply system integrating a calculation algorithm by the DYCORS method.	[37]

SWRO – Seawater reverse osmosis

(a)

(b)
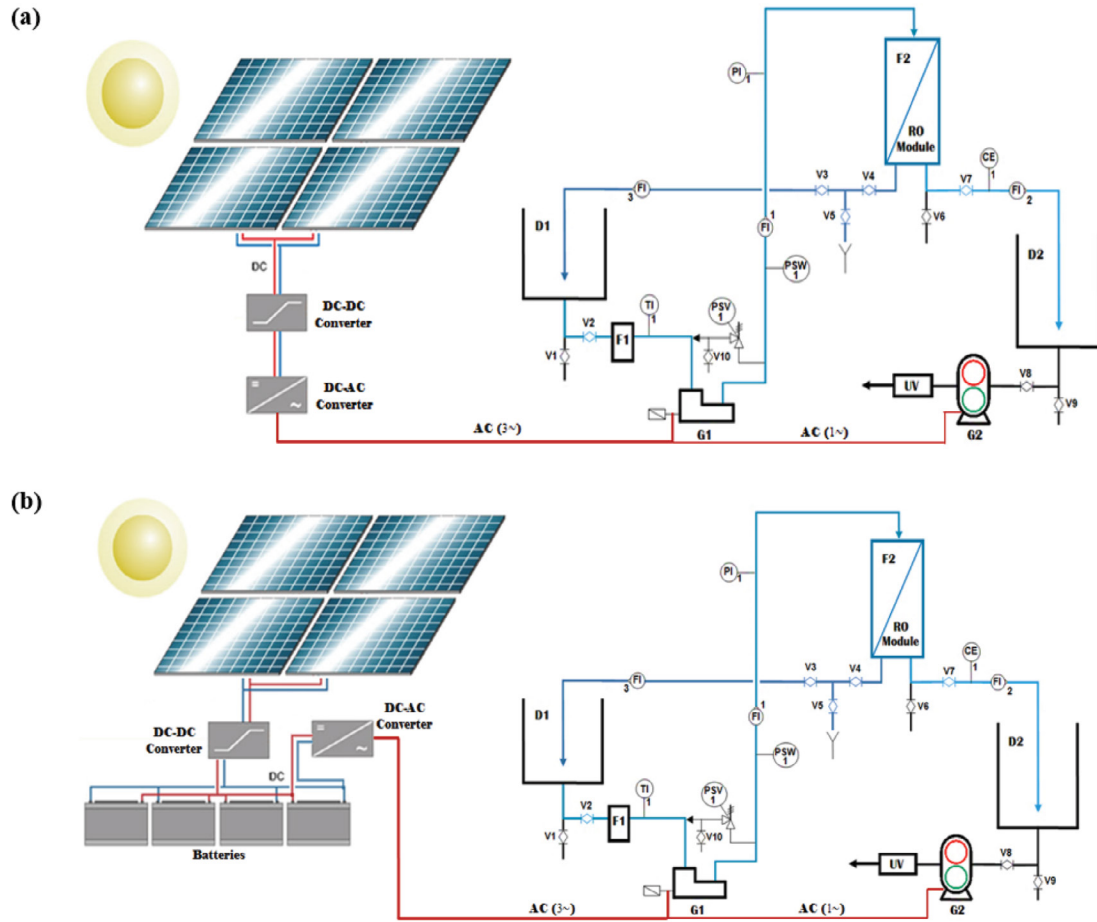
Fig. 3. (a, b) are respectively the pilot system RO/EV of the RO desalination unit powered by a photovoltaic solar source with and without batteries.
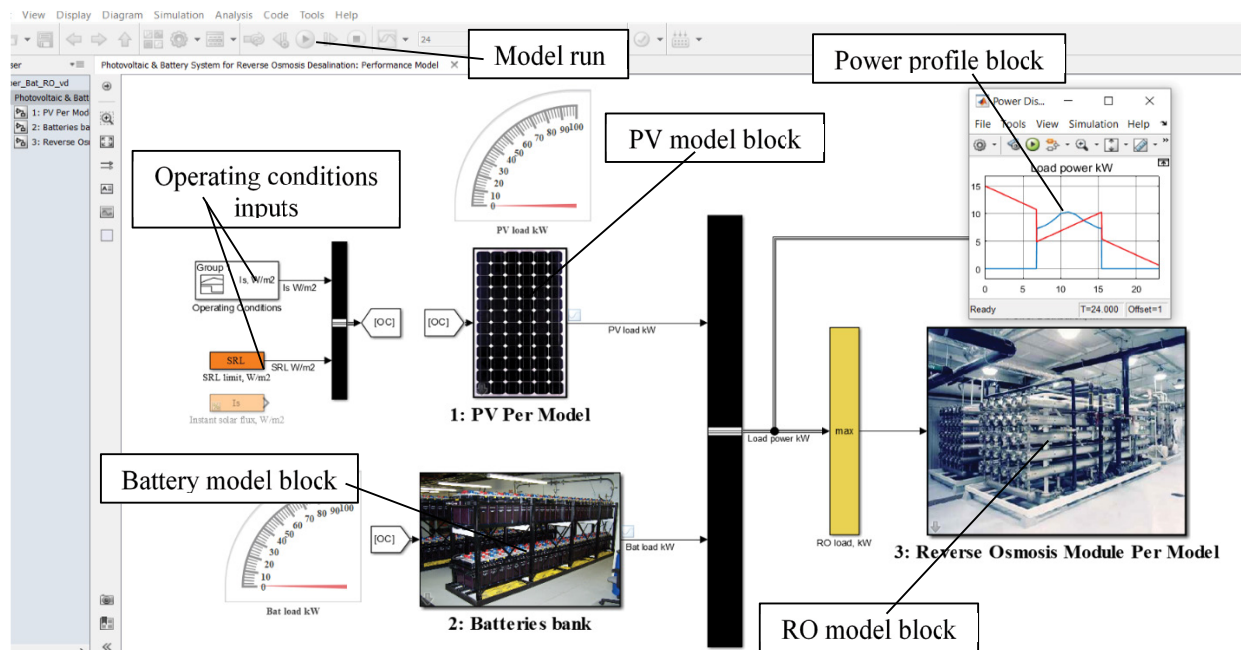

Fig. 4. The system model browser under MATLAB/Simulink environment.

The reverse saturation current module is calculated based on I_{scr}, Å, open-circuit voltage, V_{oc}, short circuit current, I_{scr}, Å, ideality factor, IF (1.2–1.6, based on PV type), electron charge, q (=1.6e-19C), number of cells in series, N_s, and the ambient temperature, T_a, °C.

$$I_{rs} = \frac{I_{scr}}{\exp\left(\dfrac{q \times V_{oc}}{N_s \times (1.3865e - 23) \times IF(T_a + 273)}\right) - 1} \tag{3}$$

$$I_{pv} = N_p \times I_{ph} - N_p \times I_o \times \exp\left(\frac{q \times \left(V_{pv} + \left(I_{pv} \times R_s\right)\right)}{N_s \times IF \times (1.3865e - 23) \times (T_a + 273)}\right) + 1 \tag{6}$$

where N_p is the number of cells in parallel, and R_s is the resistance. Thence, the PV module power can be calculated in Watt.

$$P_{pv} = V_{pv} \times I_{pv} \tag{7}$$

The module area can be calculated from cells area, A_c, m², and packing factor, B_f (~=0.89).

$$A_m = \frac{A_c \times N_s \times N_p}{B_f} \tag{8}$$

The module efficiency based on module area can be expressed as follows.

$$\eta_m = \frac{FF \times I_{scr} \times V_{oc}}{I_s \times A_m} \tag{9}$$

The total system area, m² can be calculated based on module area and number of modules (NOM).

$$A_{total} = A_m \times NOM \tag{10}$$

The total system power, Watt is then calculated.

$$P_{total} = P_{pv} \times NOM \tag{11}$$

For performance calculations, the module efficiency, the electrical efficiency, and the thermal efficiency can be calculated respectively as follows.

$$\eta_m = \frac{P_{total}}{I_s \times A_{total}} \tag{12}$$

$$\eta_{ec} = \frac{\eta_m}{B_f} \tag{13}$$

$$\eta_{th} = \frac{\eta_{ec}}{0.38} \tag{14}$$

where 0.38 is the conversion efficiency of the thermal [44].

Saturation current module, I_o, Å, can be expressed from the following relation where E_{go} is band gap (=1.1–1.6), eV.

$$I_o = I_{rs} \times \left(\frac{T_a + 273}{298}\right)^3 \times \exp\left(\frac{q \times E_{go}}{IF \times 1.3865e - 23} \times \left(\frac{1}{298} - \frac{1}{T_a + 273}\right)\right) \tag{4}$$

For the PV current, it will be assumed that V_{pv} parameter is equal to the V_{oc}, V.

$$V_{pv} = V_{oc} \tag{5}$$

4.2. Battery bank mathematical model

Concerning the power bank battery of the PV-RO system calculations, the following steps that have been adopted [45]. For the battery in discharging mode, AH should be calculated. For single battery, the AH_b is calculated based on battery current, I_b, Å, and the discharging time, t_d, h.

$$AH_b = I_b \times t_d \tag{15}$$

For single battery storage, Wh, the battery voltage V_b is multiplied by the AH_b.

$$BSp = AH_b \times V_b \tag{16}$$

Single battery power, W:

$$B_p = \frac{BSp \times DOD \times \eta_b}{OH \times NOC} \tag{17}$$

where DOD is the battery depth of discharge and OH is the operating hours, h, and NOC is the number of cloudy days. The total battery power bank, W can be obtained based on the battery power, B_p and the number of batteries, NOB.

Table 2
Specifications of the FT30 membrane

Property	Value
Membrane type	Thin-film polyamide
Permeate flow	1–10 m³/d at 55 bar
pH range	2–11
pH for washings	1–13
Surface area	2.8 m²
Rejection rate salt	99.4%
Maximum operating temperature	40°C
Maximum operating pressure	35 bar
Minimum pressure drop	1.5 bar
Free chlorine tolerance	<0.1 ppm

Table 3
Specifications of the different elements of the system

	Parameter	Name	Value
Desalination system motor, TECHTOP, Type MS2 100L4	P	Rated power	2,200 W
	V	Rated voltage	230 V
	I	Rated current	7.95 Å
	F	Rated frequency	50 Hz
	$\text{Cos}(\phi)$	Power factor	0.82
PVG at STC, AmeriSolar brand, Model AS-6P30	P_{max}	Nominal power	265 W
	V_{oc}	Open-circuit voltage	138.30 V
	I_{scr}	Short circuit current	2.98 Å
	V_{mp}	Voltage at nominal power	130.9 V
	I_{mp}	Current at nominal power	2.58 Å
	η	Module efficiency	14.29%
	Cell type	Polycrystalline	156 mm × 156 mm
	N_s	Number of PV cell in series	60
	N_p	Number of PV cell in parallel	01
Battery Hoppecke Sun power VL 2-1700 Type OPzV	V_{batt}	Nominal voltage	2 V
	C100/1.85 V	Nominal capacity	1,955 Ah
	C50/1.85 V	Capacity for a discharge in 50 h	1,870 Ah
	C24/1.83 V	Capacity for a discharge in 24 h	1,785 Ah
	Lt_{Batt}	Lifetime	1,600 cycles
	D_{Batt}	Dump	80%
	N_{Batt}	Total number of batteries of the system	15 unity
	$L \times l \times h$	Dimensions	215 mm × 277 mm × 855 mm

$$TBP = B_p \times NOB \tag{18}$$

Load current, Amp can be obtained based on the total battery power and the load voltage based on the application.

$$I_l = \frac{TBP}{V_l} \tag{19}$$

For charging mode, the same sequence will be considered, however, the charging time, t_c, h, will be assigned for the AH_b calculation.

Single battery Amp hour, AH.

$$AH_b = I_b \times t_c \tag{20}$$

4.3. Reverse osmosis mathematical model

In desalination systems, where the reverse osmosis membrane is the heart of the whole project, overcoming the filtration resistance and the osmotic pressure of the membrane system is very important to force the solid–liquid filtration phenomenon. As a result, fresh water is produced through the application of high pressure in the supply side by the high pressure motor pump according to the configuration of the RO membrane unit in addition to the quality and quantity of the production [44,46,47]. The following figure (Fig. 5) shows the principle of a RO module.

The RO model [48–50] can be expressed based on performance modelling technique where the output productivity should be calculated based on the input power to the RO. The feed flow rate, kg/s is calculated based on power load on the high-pressure pump (HPP, kW), the density, pump efficiency, and the pressure difference across the pump.

$$M_f = \frac{HPP \times \rho(T, X_f) \times \eta_p}{\Delta P} \tag{21}$$

The RO productivity, kg/s is calculated based on the assigned recovery ratio (RR) as follows.

$$M_p = RR \times M_f \tag{22}$$

The product salt concentration, g/kg is then calculated based on the feed salinity ratio, X_f, g/kg and the salt rejection percentage (SR = ~0.98).

$$X_p = X_f \times (1 - SR) \tag{23}$$

The rejected brine kg/s is the difference between the feed flow rate and the product flow rate as follows.

$$M_b = M_f - M_p \tag{24}$$

Table 4
GA model assumptions that has been considered for the proposed model

---

Population: Specifies the type of the input to the fitness function; *Type*: Double vector; *Size*: 25; *Creation function*: Constraint dependent.

Selection: The selection function chooses parents for the next generation based on their scaled values from the fitness functions; *Type*: Tournament; *Size*: 2.

Reproduction: Reproduction options determine how the genetic algorithm creates children at each new generation.

Crossover fraction: 0.8.

Mutation: Mutation functions make small random changes in the individuals in the population, which provide genetic diversity and enable the genetic algorithm to search a broader space; *Type*: Constraint dependent.

Crossover: Crossover combines two individuals, or parents, to form a new individual, or child, for the next generation; *Function type*: Intermediate; *Ratio*: 1.

Migration: Migration is the movement of individuals between subpopulations, which the algorithm creates if the case is set the population size to be a vector of length greater than 1. Every so often, the best individuals from one subpopulation replace the worst individuals in another subpopulation; *Direction*: Forward; *Fraction*: 0.2; *Interval*: 20.

Based on the mass and salt balances, the rejected salt concentration g/kg is calculated.

$$X_b = \frac{M_f \times X_f - M_p \times X_p}{M_b} \qquad (25)$$

The average salt concentration kg/m³:

$$X_{av} = \frac{M_f \times X_f + M_b \times X_b}{M_f + M_b} \qquad (26)$$

The temperature correction factor, °C:

$$\text{TCG} = \exp\left(2{,}700 \times \left(\frac{1}{T+273} - \frac{1}{298}\right)\right) \qquad (27)$$

The membrane water permeability k_w;

$$k_w = 6.84 \times 10^{-8} \times \left(18.6865 - \left(0.177 \times X_b\right)\right) / \left(T + 273\right) \qquad (28)$$

The salt permeability k_s is;

$$k_s = \text{FF} \times \text{TCF} \times 4.72 \times 10^{-7} \\ \times \left(0.06201 - \left(5.31 \times 10^{-5} \times \left(T + 273\right)\right)\right) \qquad (29)$$

where FF is the membrane-fouling factor (FF = 0.8). The calculations of osmotic pressure for feed side, brine side, and distillate product side are found as follows:

$$\Pi_f = 75.84 \times X_f \qquad (30)$$

$$\Pi_b = 75.84 \times X_b \qquad (31)$$

$$\Pi_d = 75.84 \times X_d \qquad (32)$$

The average osmotic pressure on the feed side:

$$\Pi_{av} = 0.5 \times \left(\Pi_f + \Pi_b\right) \qquad (33)$$

The net osmotic pressure across the membrane:

$$\Delta\Pi = \Pi_{av} - \Pi_d \qquad (34)$$

The net pressure difference across the membrane:

$$\Delta P = \left(\frac{M_d}{3{,}600 \times \text{TCF} \times \text{FF} \times A_e \times n_e \times N_v \times k_w}\right) + \Delta\Pi \qquad (35)$$

where A_e is the element area in m², n_e is the number of membrane elements, and N_v is the number of pressure vessels.

The specific power consumption (SPC, kWh/m³) is calculated based on the high-pressure pump (HPP, kW).

$$\text{SPC} = \frac{1{,}000 \times \text{HPP}}{3{,}600 \times M_p} \qquad (36)$$

Density, kg/m³ is calculated as presented in the following function. This equation is applicable in the salinity range of 0 to 160 g/kg and for temperature from 10°C to 180°C.

$$\rho_w = \left(\begin{array}{l} 0.5 \times a_0 + a_1 \times Y + a_2 \times \left(2 \times Y^2 - 1\right) + \\ a_3 \times \left(4 \times Y^3 - 3 \times Y\right) \end{array}\right) \times 1{,}000 \qquad (37)$$

where
$a_0 = 2.01611 + 0.115313 \times \sigma + 0.000326 \times ((2 \times (\sigma^2)) - 1)$;
$a_1 = -0.0541 + 0.001571 \times \sigma + 0.000423 \times ((2 \times (\sigma^2)) - 1)$;
$a_2 = -0.006124 + 0.00174 \times \sigma + 0.000009 \times ((2 \times (\sigma^2)) - 1)$;
$a_3 = 0.000346 + 0.00008 \times \sigma + 0.000053 \times ((2 \times (\sigma^2)) - 1)$;
$Y = 2T - 200/160$; $\sigma = (2{,}000X) - 150/150$; X (g/kg).

Specific heat capacity (J/kg°C): the specific heat of water at constant pressure is:

$$C_p = \frac{1}{1{,}000} \times \left(a_p + b_p \times T + c_p \times T^2 + d_p \times T^3\right) \qquad (38)$$

$a_p = 4{,}206.8 - 6.6197X + 1.2288 \times 10^{-2}X^2$;
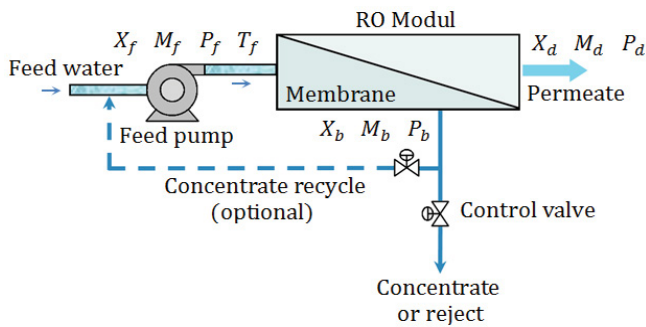$b_p = -1.1262 + 5.4178X \times 10^{-2}X - 2.2719 \times 10^{-4}X^2$;

Fig. 5. Simplified basic flow diagram of the RO process.

$c_p = 1.2026 \times 10^{-2} - 5.3566 \times 10^{-4}X + 1.8906 \times 10^{-6}X^2;$
$d_p = 6.8774 \times 10^{-7} + 1.517 \times 10^{-6}X - 4.4268 \times 10^{-9}X^2.$

4.4. Genetic algorithms of photovoltaic/RO

A genetic algorithm (GA) is a method of solving both constrained and unconstrained optimization problems based on a natural selection process that mimics biological evolution. GAs search for the optimum solution from one set of possible solutions that is an array of decision-variable values. This set of possible solutions is called a population. There are several populations in a GA run, and each of these populations is called a generation. Generally, at each new generation, better solutions (i.e., decision-variable values) that are closer to the optimum solution as compared to the previous generation are created. In the GA context, the set of possible solutions (array of decision-variable values) is defined as a chromosome, while each decision-variable value present in the chromosome is formed by genes [51]. Population size is the number of chromosomes present in a population. The GA process is briefly shown in Fig. 6. In this work, it is particularly important to assign the main GA model criteria regarding to the main process that shown in Fig. 6. The following assumptions (Table 4) are considered for the proposed GA to achieve optimum results.

To construct any GA model, the objective function for each unit should be performed. For the PV model, module power in Watt, module efficiency, total power, field power, total efficiency, and electrical efficiency. The GA would be a multi objective function model. The objective function that needed to be maximized or minimized will be assigned as $y(1,…,n)$, where the inputs that effect the function would be assigned as $x(1,…,n)$. For the PV GA model, $y(1)$ = module power, Watt, $y(2)$ = module efficiency, $y(3)$ = Total power, Watt, $y(4)$ = total efficiency, and $y(5)$ = electrical efficiency. Table 4 summarizes the main inputs and objective functions to be maximized and/or minimized for the PV system. In the same regard, Table 6 lists the objective functions for the RO unit.

5. Results and discussions

5.1. Environmental operating conditions

The studied project is installed within the faculty of sciences Aîn Chock Casablanca (Laboratory of

Renewable Energies and Dynamics Systems). Casablanca is a Moroccan city located in North Africa (Latitude L = 33.567°, Longitude l = –7.667°, Altitude H = 55 m, Climate zone = IV, 1), it is characterized by a very large share of population at national level, this explains the region's significant need for electricity and drinking water, etc. Fig. 7 presents the metrological data of the studied region. The studied region (Casablanca-Morocco) receives an annual daily solar radiation-horizontal of around 4.58 kWh/m² d (Fig. 7a and d), this daily global radiation varies from 2.70 in December to 6.40 kWh/m² d in June. According to Fig. 7b, Casablanca-Morocco is a region that has a very high sunshine duration, it varies between 5 h 54 m in December and 9 h 50 m in June (60%–70% of astronomical sunshine duration), a situation that will increase energy production during this period. Fig. 7 shows a very good presence of solar radiation at the location of operation. In fact, in September (Fig. 8), Casablanca recognizes a maximum irradiation during the whole day, however, in December, the irradiation is at its minimum value during all the year. These results are directly related to the position of the sun, and the tilt of the earth. That would give a clear indication about the importance of using PV in that regard.

6. Results and validation

At the laboratory scale of Renewable Energies and Dynamics Systems, Faculty of Sciences Ain Chock of Casablanca-Morocco, after the study that has been prepared saline water with a salinity of 2,500 ppm to desalinate it. During this study which is based on the variation of delivery pressure of the system by the main pump of the installation from 15 to 35 bar to find out their effect on the productivity of the installation. Table 7 lists some of the proposed system results against the developed software model. The results show a remarkable matching between the experimental and simulation results. For the RO results, the specific power consumption is found relatively high with a value of 8.7 kWh/m³.

That would need the optimization model to minimize the SPC to minimum levels. Decreasing the SPC would indicate that the system can produce more freshwater at low rates of power consumption. The product salinity is almost zero with maximum production rate of 5.45 m³/d. The brine loss flow rate is about 29.75~30.89 m³/d where the feed flow rate is about 35~36.34 m³/d. Thence, the recovery ratio is recorded low by 15% as a value. That would probably need an optimization in order to maximize the recovery ratio as much as possible.

Concerning the PV part, generally, the results of the simulation model are found in good matching with experimental setup. The module efficiency is about 7%–14%, the total system efficiency is about 17.35%. The photon current, PV current, and PV power is recorded as 1 Å, 2.082 Å, and 310–312 W respectively. The total PV area is about 25 m² where the average cell temperature is recorded as ~40°C. For battery part, the battery Amp-hour is about 1,700 to 1,875 AH, the battery storage is 3.75 as a maximum value, and the battery voltage is 2 V. It is very important to address the system behavior along a typical or average day in the year. For that purpose, solar radiation effect on the system results, and is

Table 5
Developed GA multi-objective functions related to the PV model optimization

Inputs:

$x(1) = A_c$, cell area, m² [0.015 … 0.024];

$x(2) = T_a$, ambient temperature, °C [25 … 35];

$x(3) = I_s$, solar radiation, W/m² [200 … 1,000];

$x(4) = V_{oc}$, open-circuit voltage, V [30 … 100];

$x(5) = I_{pv}$, PV current, À [1 … 10];

$x(6) = R_s$, resistance, ohm [1 … 1.5];

$x(7) = KI$, short-circuit coefficient, Å/°C [0.0017 … 0.0017];

$x(8) = q$, electron charge, [1.6e-19 … 1.6e-19];

$x(9) = IF$, ideality factor, [1.3 … 1.3] for polycrystalline;

$x(10) = N_s$, number of cells in series, # [60 … 60];

$x(11) = N_p$, number of cells in parallel, # [1 … 1];

$x(12) = NOM$, number of modules, # [1 … 20] depending on the case study;

$x(13) = BF$, backing factor, % [75 … 80];

$x(14) = FF$, fill factor, % [80 … 88];

$x(15) = E_{go}$, band gap, eV [1.1 … 1.6].

Outputs:

For the PV module power ($y(1)$), function (39, 40) represents the main equation where function should be maximized.

$$P_{pv} = V_{oc} \times \left(N_p \times \left(\left(0.1682 + 0.0008328 \times I_s - 0.003672 \times V_{oc} + 3.053e - 06 \times I_s \times V_{oc} + 1.562e - 05 \times V_{oc}^2 - 6.45e - 09 \times I_s \times V_{oc}^2 - 1.717e - 08 \times V_{oc}^3 + \left(KI \times (T_a + 273 - 298)\right)\right) \times (I_s / 1,000)\right)\right.$$

$$- N_p \times \left(\frac{0.1682 + 0.0008328 \times I_s - 0.003672 \times V_{oc} + 3.053e - 06 \times I_s \times V_{oc} + 1.562e - 05 \times V_{oc}^2 - 6.45e - 09 \times I_s \times V_{oc}^2 - 1.717e - 08 \times V_{oc}^3}{\exp\left(\frac{q \times V_{oc}}{N_s \times (1.3865e - 23) \times IF \times (T_a + 273)}\right) - 1}\right)$$

$$\times \left((T_a + 273) / 298\right)^3 \times \exp\left(\left(\frac{q \times E_{go}}{IF \times 1.3865e - 23}\right) \times \left(\left(\frac{1}{298}\right) - \left(\frac{1}{T_a + 273}\right)\right)\right) \times \exp\left(\frac{q \times (V_{oc} + (I_{pv} \times R_s))}{N_s \times IF \times (1.3865e - 23) \times (T_a + 273)}\right) - 1$$

$$x(11) \times \left(\left(\left(0.1682 + 0.0008328 \times x(3) - 0.003672 \times x(4) + 3.053e - 06 \times x(3) \times x(4)^2 - 1.717e - 08 \times x(4)^3\right) + \times \left(\frac{x(3)}{1,000}\right)\right)\right)$$

$$x(7) \times (x(2) + 273 - 298))$$

(39)

$$y(1) = x(4) \times \left(\frac{0.1682 + 0.0008328 \times x(3) - 0.003672 \times x(4) + 3.053e - 06 \times x(3) \times x(4) + 1.562e - 05 \times x(4)^2 - 6.45e - 09 \times x(3) \times x(4)^2 - 1.717e - 08 \times x(4)^3}{\exp\left(\frac{x(8) \times x(4)}{x(10) \times (1.3865e - 23) \times x(9) \times (x(2) + 273)}\right) - 1} \right.$$

$$- x(11) \times \left(\frac{0.1682 + 0.0008328 \times x(3) - 0.003672 \times x(4) + 3.053e - 06 \times x(3) \times x(4)^2 - 6.45e - 09 \times x(3) \times x(4)^2 - 1.717e - 08 \times x(4)^3}{\exp\left(\frac{x(8) \times x(4)}{x(10) \times (1.3865e - 23) \times x(9) \times (x(2) + 273)}\right) - 1}\right)$$

$$\times \left(\frac{x(2) + 273}{298}\right)^3 \times \exp\left(\left(\frac{x(8) \times x(15)}{x(9) \times 1.3865e - 23}\right) \times \left(\left(\frac{1}{298}\right) - \left(\frac{1}{x(2) + 273}\right)\right)\right) \times \exp\left(\frac{x(8) \times (x(4) + (x(5) \times x(6)))}{x(10) \times x(9) \times (1.3865e - 23) \times (x(2) + 273)}\right) - 1$$

(40)

Table 5

The objective function (maximization) of the module efficiency (y(2)) can be calculated based on functions (41, and 42) as following:

$$\eta_m = \frac{\mathrm{FF} \times \left(0.1682 + 0.0008328 \times I_s - 0.003672 \times V_{oc} + 3.053e-06 \times I_s \times V_{oc} + 1.562e-05 \times V_{oc}^2 - 6.45e-09 \times I_s \times V_{oc}^2 - 1.717e-08 \times V_{oc}^3\right) \times V_{oc}}{I_s \times \left(\dfrac{A_c \times N_s \times N_p}{B_f}\right)}$$

(41)

$$y(2) = \frac{x(14) \times \left(0.1682 + 0.0008328 \times x(3) - 0.003672 \times x(4) + 3.053e-06 \times x(3) \times x(4) + 1.562e-05 \times x(4)^2 - 6.45e-09 \times x(3) \times x(4)^2 - 1.717e-08 \times x(4)^3\right) \times x(4)}{x(3) \times \left(\dfrac{x(1) \times x(10) \times x(11)}{x(13)}\right)}$$

(42)

Total objective function for the total system power (y(3)), Watt, is presented as follows:

$$P_{\text{total}} = V_{oc} \times \left(\left(N_p \times \left(\left(\left(0.1682 + 0.0008328 \times I_s - 0.003672 \times V_{oc} + 3.053e-06 \times I_s \times V_{oc} + 1.562e-05 \times V_{oc}^2 - 6.45e-09 \times I_s \times V_{oc}^2 - 1.717e-08 \times V_{oc}^3\right) + \left(\mathrm{K1} \times (T_a + 273 - 298)\right)\right) \times \left(\frac{I_s}{1,000}\right)\right)\right) \right.$$
$$- N_p \times \left[\frac{0.1682 + 0.0008328 \times I_s - 0.003672 \times V_{oc} + 3.053e-06 \times I_s \times V_{oc} + 1.562e-05 \times V_{oc}^2 - 6.45e-09 \times I_s \times V_{oc}^2 - 1.717e-08 \times V_{oc}^3}{\exp\left(\frac{q \times V_{oc}}{N_s \times (1.3865e-23) \times \mathrm{IF} \times (T_a + 273)}\right) - 1}\right] \times \left(\frac{T_a + 273}{298}\right)^3 \times \exp\left(\left(\frac{q \times E_{go}}{\mathrm{IF} \times 1.3865e-23}\right) \times \left(\left(\frac{1}{298}\right) - \left(\frac{1}{T_a + 273}\right)\right)\right) \times \exp\left(\frac{q \times \left(V_{oc} + (I_{pv} \times R_s)\right)}{N_s \times \mathrm{IF} \times (1.3865e-23) \times (T_a + 273)}\right) - 1 \right) \times \mathrm{NOM}$$

(43)

$y(3) = (x(4) \times ((x(11) \times (((0.1682 + 0.0008328 \times x(3) - 0.003672 \times x(4) + 3.053e-06 \times x(3) \times x(4) + 1.562e-05 \times x(4)^2 - 6.45e-09 \times x(3) \times x(4)^2 - 1.717e-08 \times x(4)^3) + (x(7) \times (x(2) + 273 - 298)) \times (x(3)/1,000))) - (x(11) \times (((0.1682 + 0.0008328 \times x(3) - 0.003672 \times x(4) + 3.053e-06 \times x(3) \times x(4) + 1.562e-05 \times x(4)^2 - 6.45e-09 \times x(3) \times x(4)^2 - 1.717e-08 \times x(4)^3)/(\exp(x(8) \times x(4))/(x(10) \times (1.3865e-23) \times x(9) \times x(2) + 273)) - 1) \times (x(2) + 273/298)^3 \times \exp(((x(8) \times x(15))/(x(9) \times 1.3865e-23) \times ((1/298) - (1/(x(2) + 273))) \times \exp((x(8) \times ((x(4)) + (x(5) \times x(6)))/(x(10) \times x(9) \times (1.3865e-23) \times (x(2) + 273))) - 1))) \times x(12)$

(44)

For the overall or total efficiency ($y(4)$), the following objective function is performed.

$$\eta_t = ((V_{oc} \times ((N_p \times (((0.1682 + 0.0008328 \times I_s - 0.003672 \times V_{oc} + 3.053e - 06 \times I_s \times V_{oc} + 1.562e - 05 \times V_{oc}^2 - 6.45e - 09 \times I_s \times V_{oc}^2 - 1.717e - 08 \times V_{oc}^3) + (KI \times (T_a + 273 - 298)) \times (I/1,000))) - (N_p \times (((0.1682 + 0.0008328 \times I_s - 0.003672 \times V_{oc} + 3.053e - 06 \times I_s \times V_{oc} + 1.562e - 05 \times V_{oc}^2 - 6.45e - 09 \times I_s \times V_{oc}^2 - 1.717e - 08 \times V_{oc}^3)/(\exp((q \times V_{oc})/(N_s^t \times (1.3865e - 23) \times IF \times (T_a + 273))) - 1)) \times ((T_a + 273)/298)^3 \times \exp(((q \times E_{go})/(IF \times 1.3865e - 23) \times ((1/298) - (1/(T_a + 273)))) \times \exp((q \times (V_{oc} + (I_{pv} \times R_s)))/(N_s \times IF \times (1.3865e - 23) \times (T_a + 273))) - 1)) \times NOM)/(I_s \times (((A_c \times N_s \times N_p)/B_f) \times NOM))$$ (45)

$$y(4) = ((x(4) \times ((x(11) \times (((0.1682 + 0.0008328 \times x(3) - 0.003672 \times x(4) + 3.053e - 06 \times x(3) \times x(4) + 1.562e - 05 \times x(4)^2 - 6.45e - 09 \times x(3) \times x(4)^2 - 1.717e - 08 \times x(4)^3 + (x(7) \times (x(2) + 273 - 298)) \times (x(3)/1,000))) - (x(11) \times (((0.1682 + 0.0008328 \times x(3) - 0.003672 \times x(4) + 3.053e - 06 \times x(3) \times x(4) + 1.562e - 05 \times x(4)^2 - 6.45e - 09 \times x(3) \times x(4)^2 - 1.717e - 08 \times x(4)^3)/(\exp((x(8) \times x(4))/(x(10) \times (1.3865e - 23) \times x(9) \times (x(2) + 273))) - 1)) \times ((x(2) + 273)/298)^3 \times \exp(((x(8) \times x(15))/(x(9) \times 1.3865e - 23) \times ((1/298) - (1/(x(2) + 273))))) \times \exp((x(8) \times ((x(4) + (x(5) \times x(6))))/(x(10) \times x(9) \times (1.3865e - 23) \times x(2) + 273))) - 1)))/(x(3) \times (((x(1) \times x(10) \times x(11))/x(13)) \times x(12))))$$ (46)

The objective function for the electrical efficiency ($y(5)$):

$$\eta_{ec} = \frac{FF \times (0.1682 + 0.0008328 \times I_s - 0.003672 \times V_{oc} + 3.053e - 06 \times I_s \times V_{oc} + 1.562e - 05 \times V_{oc}^2 - 6.45e - 09 \times I_s \times V_{oc}^2 - 1.717e - 08 \times V_{oc}^3) \times V_{oc}}{I_s \times \left(\dfrac{A_c \times N_s \times N_p}{B_f}\right) B_f}$$ (47)

$$y(5) = \frac{x(14) \times \left(0.1682 + 0.0008328 \times x(3) - 0.003672 \times x(4) + 3.053e - 06 \times x(3) \times x(4) + 1.562e - 05 \times x(4)^2 - 6.45e - 09 \times x(3) \times x(4)^2 - 1.717e - 08 \times x(4)^3\right) \times x(4)}{x(3) \times \left(\dfrac{x(1) \times x(10) \times x(11)}{x(13)}\right)}{x(13)}$$ (48)

Table 6
Developed GA multi-objective functions related to the RO model optimization

Inputs:

$x(1)$ = HPP, high-pressure pump power, kW [PV output];

$x(2)$ = η_p, pump efficiency, % [75 …85];

$x(3)$ = d_p, pressure drop, kPa [1,500 … 3,500];

$x(4)$ = T_f, feed temperature, °C [25 …40];

$x(5)$ = X_f, feed salinity ratio, g/kg [1 …4];

$x(6)$ = RR, recovery ratio, % [10 …20];

$x(7)$ = SR, salt rejection, % [98.5 …99.1].

Outputs:

The RO productivity, kg/s can be obtained by the following objective function ($y(1)$, maximization).

$$M_p = RR \times ((HPP \times ((0.5 \times (2.01611 + 0.115313 \times ((2 \times X_f) - 150)/150) + 0.000326 \times ((2 \times (((2 \times X_f) - 150)/150)^2 - 1)) + (-0.0541 + 0.001571 \times (((2 \times X_f) - 150)/150) + 0.000423 \times ((2 \times (((2 \times X_f) - 150)/150)^2 - 1)) \times (((2 \times T_f) - 200)/160) + (-0.006124 + 0.00174 \times (((2 \times X_f) - 150)/150) + 0.000009 \times (2 \times (((2 \times X_f) - 150)/150)^2 - 1)) \times (2 \times (((2 \times T_f) - 200)/160)^2 - 1) + (0.000346 + 0.000087 \times (((2 \times X_f) - 150)/150) + 0.000053 \times ((2 \times (((2 \times X_f) - 150)/150)^2 - 1)) \times (4 \times (((2 \times T_f) - 200)/160)^3 - 3 \times (((2 \times T_f) - 200)/160))) \times 1,000) \times \eta_p)/\Delta P) \tag{49}$$

$$y(1) = x(6) \times ((x(1) \times ((0.5 \times (2.01611 + 0.115313 \times ((2 \times x(5)) - 150)/150) + 0.000326 \times (2 \times (((2 \times x(5)) - 150)/150)^2 - 1)) + (-0.0541 + 0.001571 \times (((2 \times x(5)) - 150)/150) + 0.000423 \times (2 \times (((2 \times x(5)) - 150)/150)^2 - 1)) \times (((2 \times x(4)) - 200)/160) + (-0.006124 + 0.00174 \times (((2 \times x(5)) - 150)/150) + 0.000009 \times (2 \times (((2 \times x(5)) - 150)/150)^2 - 1)) \times (2 \times (((2 \times x(4)) - 200)/160)^2 - 1) + (0.000346 + 0.000087 \times (((2 \times x(5)) - 150)/150) + 0.000053 \times ((2 \times (((2 \times x(5)) - 150)/150)^2 - 1)) \times (4 \times (((2 \times x(4)) - 200)/160)^3 - 3 \times (((2 \times x(4)) - 200)/160))) \times 1,000) \times x(2))/x(3)) \tag{50}$$

The permeate salt concentration function ($y(2)$), g/kg is obtained as following.

$$X_p = X_f \times (1 - SR) \tag{51}$$

$$y(2) = x(5) \times (1 - x(7)) \tag{52}$$

Specific power consumption, kWh/m³, objective function ($y(3)$, minimization) is obtained as following.

$$SPC = (1,000 \times HPP)/((RR \times ((HPP \times ((0.5 \times (2.01611 + 0.115313 \times (((2 \times X_f) - 150)/150) + 0.000326 \times ((2 \times (((2 \times X_f) - 150)/150)^2) - 1)) + (-0.0541 + 0.001571 \times (((2 \times X_f) - 150)/150) + 0.000423 \times ((2 \times (((2 \times X_f) - 150)/150)^2) - 1)) \times (((2 \times T_f) - 200)/160) + (-0.006124 + 0.00174 \times (((2 \times X_f) - 150)/150) + 0.000009 \times ((2 \times (((2 \times X_f) - 150)/150)^2) - 1)) \times (2 \times (((2 \times T_f) - 200)/160)^2 - 1) + (0.000346 + 0.000087 \times (((2 \times X_f) - 150)/150) + 0.000053 \times ((2 \times (((2 \times X_f) - 150)/150)^2) - 1)) \times (4 \times (((2 \times T_f) - 200)/160)^3 - 3 \times (((2 \times T_f) - 200)/160))) \times 1,000) \times \eta_p)/\Delta P)) \times 3,600) \tag{53}$$

$$y(3) = (1,000 \times x(1))/((x(6) \times ((x(1) \times ((0.5 \times (2.01611 + 0.115313 \times (((2 \times x(5)) - 150)/150) + 0.000326 \times ((2 \times (((2 \times x(5)) - 150)/150)^2) - 1)) + (-0.0541 + 0.001571 \times (((2 \times x(5)) - 150)/150) + 0.000423 \times ((2 \times (((2 \times x(5)) - 150)/150)^2) - 1)) \times (((2 \times x(4)) - 200)/160) + (-0.006124 + 0.00174 \times (((2 \times x(5)) - 150)/150) + 0.000009 \times ((2 \times (((2 \times x(5)) - 150)/150)^2) - 1)) \times (2 \times (((2 \times x(4)) - 200)/160)^2 - 1) + (0.000346 + 0.000087 \times (((2 \times x(5)) - 150)/150) + 0.000053 \times ((2 \times (((2 \times x(5)) - 150)/150)^2) - 1)) \times (4 \times (((2 \times x(4)) - 200)/160)^3 - 3 \times (((2 \times x(4)) - 200)/160))) \times 1,000) \times x(2))/x(3))) \times 3,600) \tag{54}$$
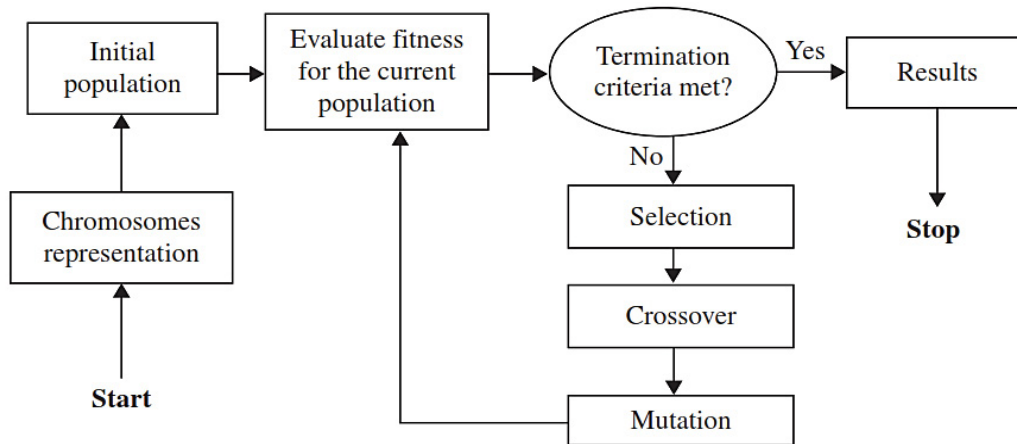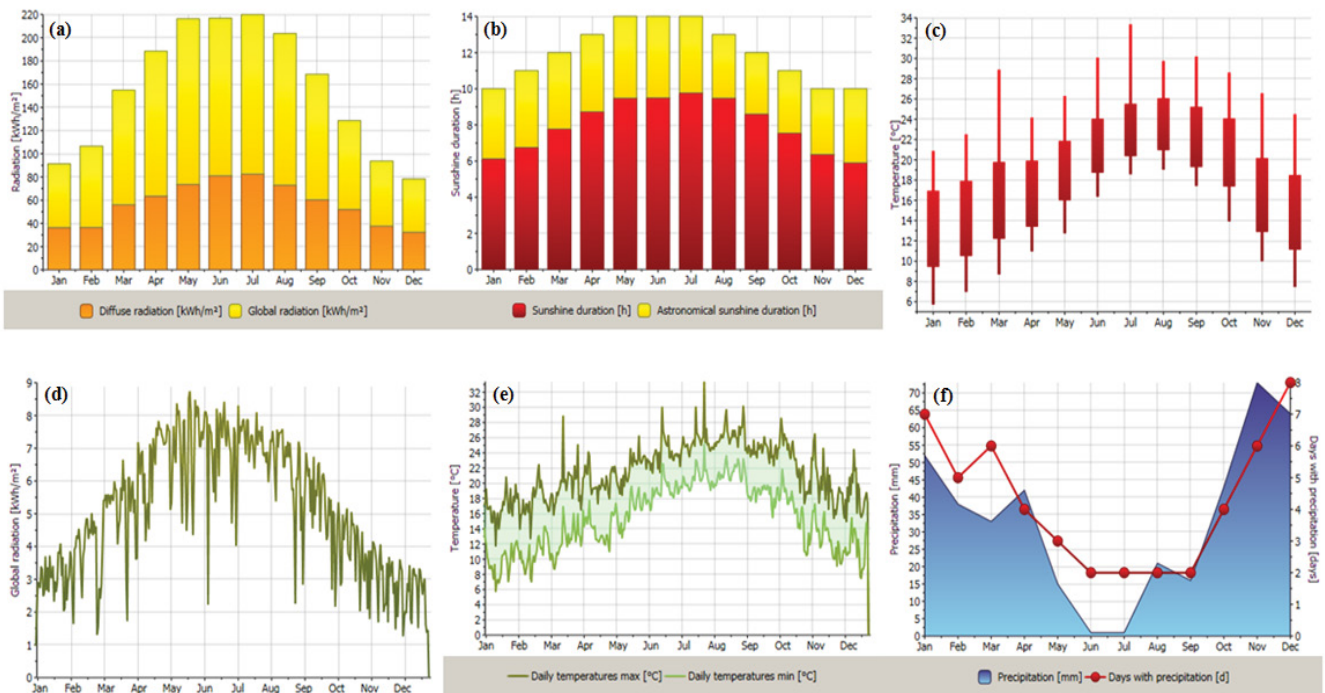
Fig. 6. The overall GA operational process [51].

Fig. 7. (a) Monthly radiation, kWh/m² (diffuse and global). (b) Sunshine duration, h. (c) Monthly temperature, °C. (d) Daily global radiation, kWh/m². (e) Daily temperature, °C. (f) Precipitation, mm and days with precipitation, d.

considered as an important power conversion parameter. Fig. 9 represents the feed flow rate daily variation during the 24 h, m³/d, brine flow rate, m³/d, product flow rate, m³/d, and product salinity, ppm of the RO unite based on different seasons (Mar, Jun, Sep, and Dec). According to Fig. 9a, the feed flow rate of the RO system is considered as a low value in December ~60 m³/d at noon compared to the other seasons, however in September, the flow rate is considered as a high value at noon (~70 m³/d) where the irradiation, I_s, is maximal. Consequently, the daily irradiation of the studied area influences directly the feed flow rate of the RO system, therefore, a high irradiation, notably at solar noon, gives a feed flow rate too, and the reverse versa. Throughout the day, the brine flow rate produced, m³/d, by the RO unit

(Fig. 9b), varies according to the variation of the irradiation. A value of ~60 m³/d is recorded at solar noon in September. Consequently, when the irradiation, I_s, W/m², is maximum, the brine flow rate produced becomes maximum as well, and the reverse is true. Fig. 9c represents clearly the product flow rate variation, m³/d during the day. It has been noticed that this variation is assimilated to feed and brine flow rates, and is obviously clear that the product flow rate is more important than brine flow rate. Thence, the result of recovery ratio, RR, % of the desalination membrane used in this study (RR = 15%). In case the product flow rate has a maximum value, the salinity, ppm of the latter becomes very low (0.0025 ppm), Fig. 9d. For that reason in sunshine period, when the solar PV field produces the electric power, the product flow

Table 7
Data results for the proposed model vs. the experimental data at the location of operation

Parameter	Simulation results	Experimental results
Power recovery	Batteries	Batteries
Solar radiation, W/m²	1,000	1,000
Operating hours, h	24	24
Feed temperature, °C	25	25
RO results		
SPC, kWh/m³	8.73	–
Power, kW	1.983	~2
Feed, m³/d	36.34	35
Brine, m³/d	30.89	29.75
Productivity, m³/d	5.452	5.25
Feed salinity, g/kg	2.5	2.5
Brine salinity, g/kg	2.941	–
Average brine salinity, g/kg	2.703	–
Freshwater salinity, ppm	0.002064~0.0	00
Feed pressure, kPa	4,000	3,800~4,000
Net osmotic pressure, kPa	206.3	–
Recovery ratio, %	15	15
Salt rejection, %	99.89	99.89
Number of pressure vessels, #	1	1
Number of elements/vessels, #	1	1
PV results		
Module efficiency/electrical efficiency, %/%	7.09/9.37	14.29/–
Overall efficiency, %	17.35	–
Total system area, m²	25.2	25.2
Photon current, Å	1.082	1
PV current, Å	2.082	2.38
PV power, W	312	310
Battery results		
Battery type, Volt	2	2
Battery efficiency, %	75	75
Battery storage, kWh	3.75	3.570
Battery amp·hour, AH	1,875	1,785~1,800
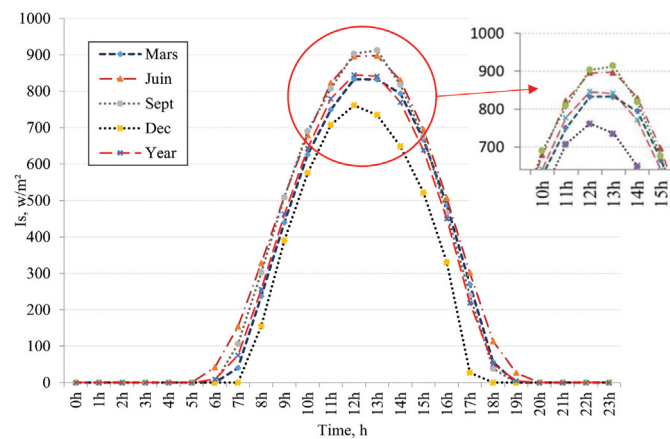
Fig. 8. The variation of the average daily irradiation of 11 y (from 2005 to 2016) of the zone studied for the months March, June, September, and December.
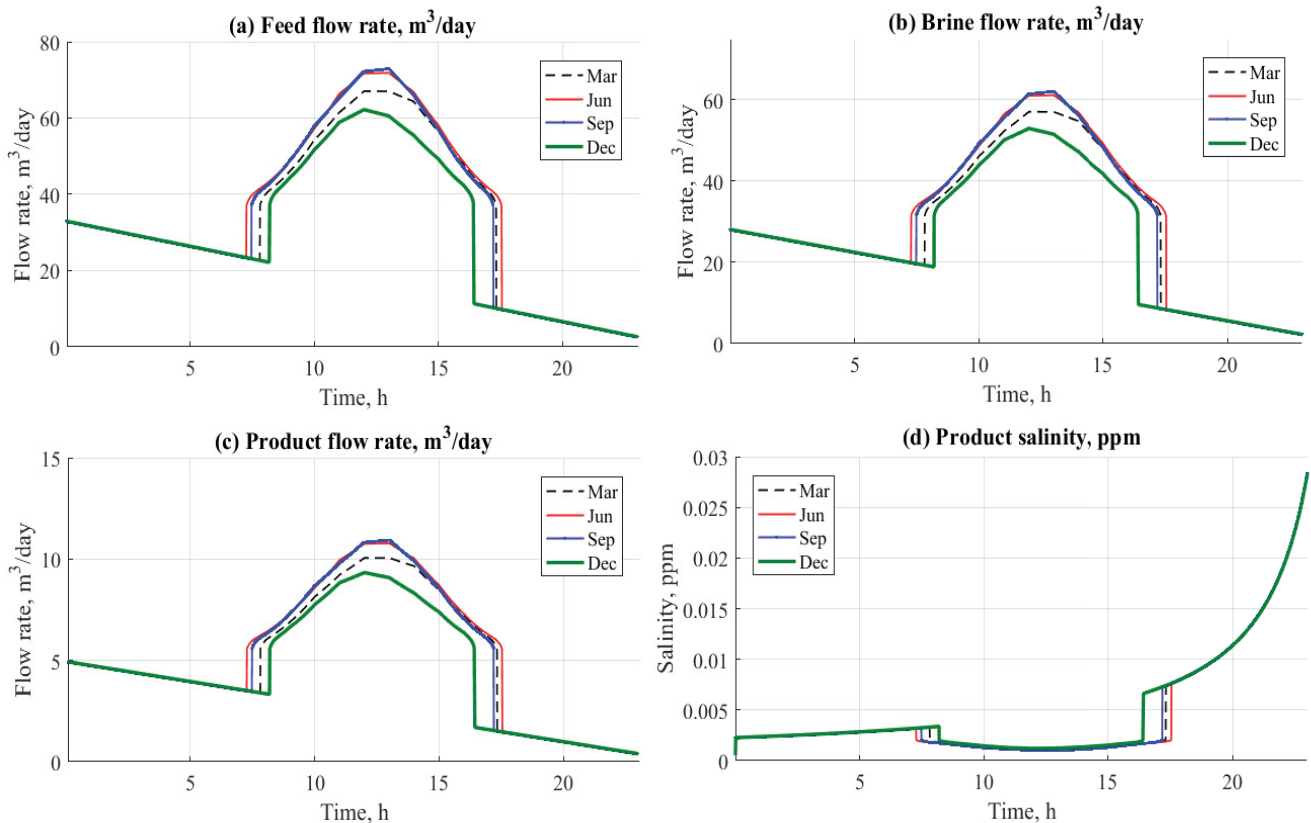
Fig. 9. Results of the RO system along 24 h based on different seasons (Mar, Jun, Sep, and Dec) for (a) feed flow rate, (b) brine flow rate, (c) product flow rate, and (d) product salinity.

rate becomes essential, consequently, their salinity becomes minimal compared with the period when the desalination system consumes the power stored in the batteries (between 0–7 h and 18–23 h). Fig. 9d shows that by reducing the power (low rates of solar radiation), the product salinity would increase slightly due to decrease of system productivity. Fig. 10 represents the daily variation of photon current during 24 h, A, module efficiency, %, electrical efficiency, % and total PV power, kW of the solar system PV based on different seasons (Mar, Jun, Sep, and Dec). According to Fig. 10a, the generation of the photonic current by the PV system in September recognized a very high value compared to the other months, particularly in December which recognize a minimum generation of this current where the irradiation, I_s, is minimal. Consequently, the daily irradiation of the studied area influences directly the generation of the photonic current of the PV system [Eq. (2)], therefore, the high irradiation (at solar noon) generates a high photon current, and the reverse is true. Throughout the day, the module efficiency of our installation (Fig. 10b), varies according to the variation of the irradiation of each season, a value of ~8% is recorded at solar noon in September which is very close to the maximum efficiency (9.37%), in December, the solar PV field works with a minimum efficiency, it is observed that the positioning and the sun inclinations have a direct effect on the efficiency, consequently, the moment when the irradiation, I_s, W/m², is perpendicular to the PV solar cell (at solar noon), the efficiency of the latter becomes maximum, and

the reverse is true. Fig. 10c represents perfectly the electrical efficiency variation during the day, it is clearly noticed that this variation is assimilated to that of module efficiency, this confirms that the module efficiency influences the electrical efficiency of the PV production. That is to say a convection efficiency maximum value is recorded at solar noon in September, this value is quite close to 10%. It is also noticed that at solar noon, the overall efficiency of the PV system is always at its maximum regardless the season (Mar, Jun, Sep, and Dec), for this reason, the power production of PV system recognize a maximum value at solar noon as well (Fig. 10d), in fact, the quantity of power, kW, produced by the PV field was recorded during June, this production is largely linked to the duration of sunshine, where June recognized a very important duration of sunshine in Casablanca comparing to other months. Generally, the PV efficiency found is low according to the use of polycrystalline type. Fig. 11 represents the daily variation along 24 h of the battery load current, A, and PV/Battery power profile, kW, based on different seasons (Mar, Jun, Sep, and Dec). According to Fig. 11a, the battery load current of the power bank, recognized a remarkable decrease during the period of 00–07 h, in this period, the PV system didn't produce any power, on the other hand the RO unit produced fresh water. In effect, the power consumed by the desalination system is that stored in the battery bank. For the period from 7–18 h, the current of the battery starts to increase, this increase means that the storage system starts to charge from the power produced by

Table 8
GA index depending on the high production rate, m³/d

Optimum output					Best individuals' variables					
M_p, kg/s	X_p, g/kg	M_b, kg/s	SPC, kWh/m³	Power, kW	η	d_p, kPa	T_f, °C	X_f, g/kg	RR	SR
0.422	**0.022244**	**1.716**	**2.658**	**4.041**	**0.8**	**1,508.037**	**26.081**	**2.044643**	**0.19748**	**0.9891**
0.305	0.020669	1.265	2.695	2.962	0.8	1,505.313	25.845	2.039428	0.19441	0.9898
0.194	0.020252	0.833	2.861	2.002	0.8	1,555.204	25.526	2.018716	0.18914	0.9899
0.157	0.024086	0.628	2.609	1.476	0.8	1,500	25.001	2.016724	0.20000	0.9880
0.091	0.023573	0.432	6.203	2.047	0.8	3,108.202	35.144	2.053011	0.17491	0.9885
0.052	0.057796	0.225	3.880	0.726	0.8	2,093.031	25.103	2.959391	0.18754	0.9805
0.015	0.031963	0.066	9.903	0.535	0.8	5,259.15	35.598	2.1487	0.18541	0.9851
0.012	0.031791	0.069	12.250	0.545	0.8	5,294.922	35.463	2.166238	0.15091	0.9853
0.012	**0.032005**	**0.069**	**12.247**	**0.541**	**0.8**	**5,292.256**	**35.491**	**2.164365**	**0.15086**	**0.9852**
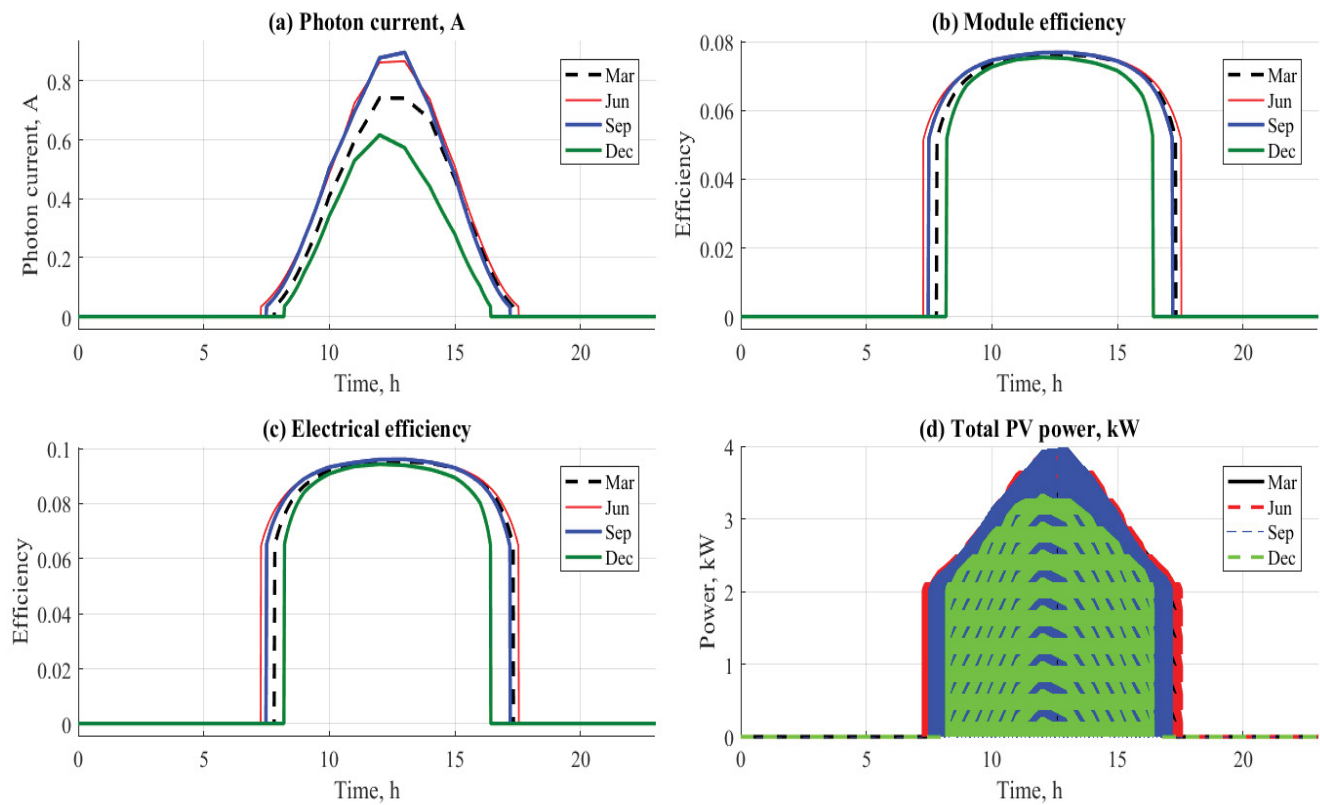
Fig. 10. Results of the PV system along 24 h based on different seasons (Mar, Jun, Sep, and Dec) for (a) photon current, (b) module efficiency, (c) electrical efficiency, and (d) rated power.

the solar field, the power generated by the PV system is not fully stored in the battery bank, a large part of this power is exploited directly by the desalination unit (Fig. 11b), this is the reason that the production of the RO system is at its maximum as the electrical power is maximum as well (Fig. 9c). For the period from 18–23 h, the PV system did not produce any power, therefore, the RO unit will consume the power from the battery, for this reason that the working characteristic of the power bank is: discharge-charge-discharge as it is perfectly presented in the figure Fig. 11b.

6.1. Optimization results

It is aimed to optimize the system performance (productivity) for the maximum gain with low power consumption. For that purpose, GA is implemented to recognize the best operating conditions to enhance the system productivity. Based on Tables 4–6, the GA model results are presented. Fig. 12 shows the GA model results based on the generations fitness and objectives of the RO system. The average distance between individual parameters is found
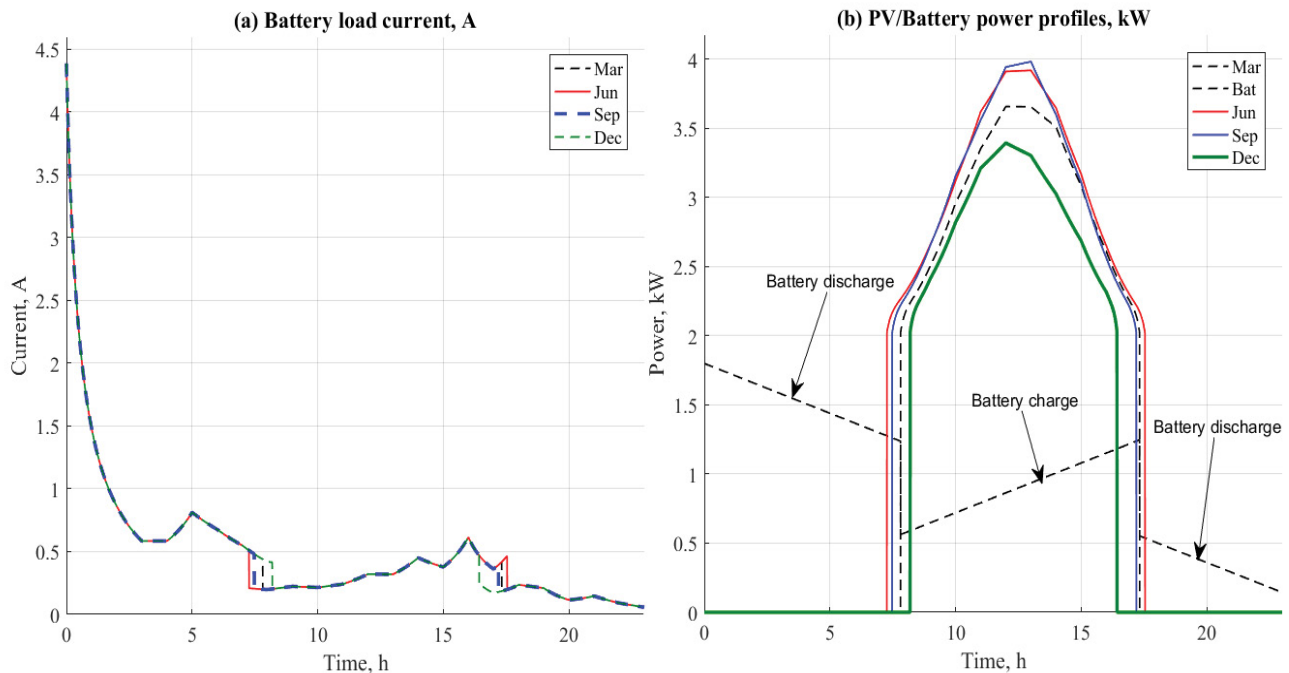
Fig. 11. Results of the battery bank along 24 h based on different seasons (Mar, Jun, Sep, and Dec) for (a) battery load current and (b) power profile.

in the range between 1,000 and 2,500 along 140 generations. That would improve accuracy of the GA model. It is observed from the histogram (Fig. 12b) that the bin width is too small because it showed too much individual data and did not allow the underlying pattern of the data to be easily seen. Table 8 indexed the best operating conditions for the RO objective functions (M_p, X_p, M_b, SPC). For maximum productivity, the power is about 4.04 kW, the feed temperature should be 26.0811°C, the pressure should be 1,508.03 kPa, the feed salinity should be 2.044 g/kg, RR is 0.19748 and the SR is 0.9891. That also would result a low SPC which is highly recommended. Lowering the power consumption of the RO would reduce the load demand on the PV modules. The SPC is remarkably about 2.658 kWh/m³. The lowest production rate is combined with high SPC where the M_p = 0.0122 m³/d and the SPC = 12.24 kWh/m³.

Fig. 13 represents the effect of optimization results by GA of power and pressure drop on the productivity, m³/d, product salinity, ppm, feed flow rate, m³/d, and SPC, kWh/m³ in case of increasing the range of the operating conditions. The result data on the Fig. 13 has been recorded based on 15% of recovery ratio and 2.5 g/kg of feed salinity ratio. Fig. 13a shows that by increasing the power P (range = 0.5–6 kW), the productivity, m³/d will increase as well. For instance, at pressure drop d_p = 1,500 kPa and the power P = 0.5 kW, the productivity was recorded as ~2.5 m³/d. However, at P = 6 kW and pressure drop d_p = 1,500 kPa, and the productivity is equal to ~40 m³/d, with a very important percentage of increasing.

Therefore, it will be highly recommended to operate the system at low pressure drop and high power. The reason why reducing the pressure drop will increase the operating power of the desalination system. However, increasing the

power P, kW, would increase the productivity, m³/d. Both parameters have a direct effect on the production flow rate of fresh water to choose the most adopted operating mode. Consequently, it is highly recommended to assign the pressure drop at a value of 1,500 kPa and power at a value of 4–6 kW to achieve maximum productivity, m³/d (~40). Fig. 13b shows that by increasing the pressure drop, the product salinity, ppm, will increase too. Increasing the product salinity is not favorable; however, it will reduce the fresh water quality produced and their cost values too.

Therefore, to obtain a suitable freshwater flow rates, m³/d, with minimum ranges of pressure drop, kPa and feed flow rate, m³/d (Fig. 13c). Reducing the power will increase the product salinity too. However, it will reduce the productivity, m³/d, and feed flow rate, m³/d parameters as well (Fig. 13c and b). The pressure drop will also cause a massive reduce in feed flow rate and productivity. For instance, the percentage decrease and will become 99.84% at d_p = 1,500 kPa (from 300 up to 25 m³/d). However, the variation of all these parameters will influence the SPC, kWh/m³ (Fig. 13d). The variation of the power in the system has no effect on SPC, kWh/m³, on the other hand the pressure drop has a direct effect on it. If we manage to minimize the pressure drop, the SPC also becomes minimal, the thing that will reduce the rating production of fresh water with good quality production (<0.003 ppm).

Fig. 14 represents the effect of optimization results by GA of power and feed salinity ratio on the productivity, m³/d, product salinity, g/kg, feed flow rate, m³/d, and SPC, kWh/m³. The result data in Fig. 14 has been recorded based on 15% of recovery ratio and 3,500 kPa as an average value of the pressure drop. Fig. 14a shows that by increasing the power P (range = 0.5–6 kW), the productivity, m³/d, would increase
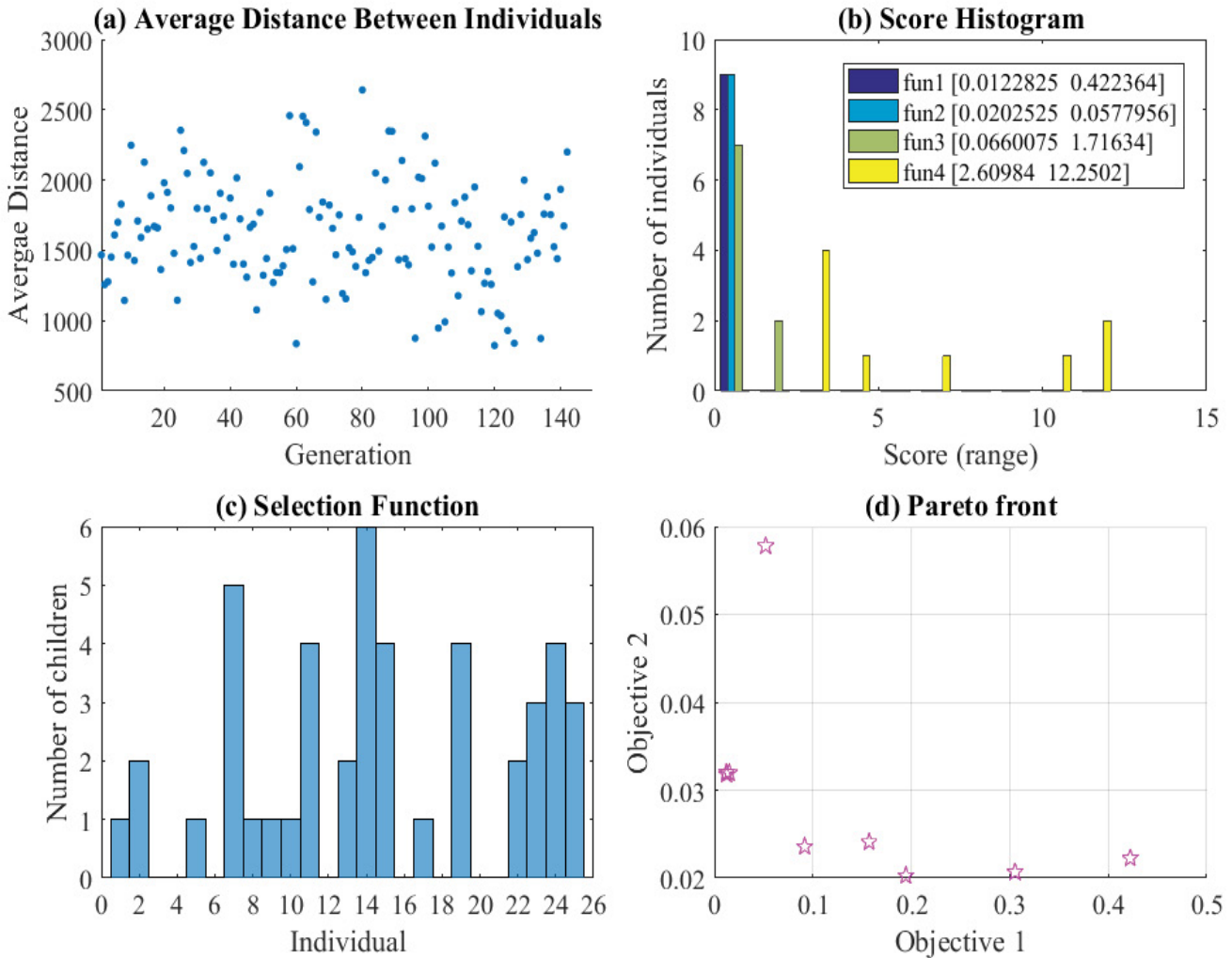
Fig. 12. GA fitness results according to RO objective functions: (a) average distance between individuals, (b) score histogram, (c) selection function and (d) Pareto front.

too as anticipated. For instance, at product salinity X_f = 2.5 g/kg and the power P = 0.5 kW, the productivity is recorded as ~2 m³/d. However, at P = 6 kW and product salinity X_f = 2.5 g/kg, the productivity is equal to ~14 m³/d. Consequently, it is clearly noticed that the productivity of the desalination system, in this case, does not depend on the feed salinity ratio X_f. Certainly, it has a slight effect regarding to water density but cannot change the production behavior. However, it is strongly linked to the high power. Fig. 14b shows that by increasing the feed salinity ratio, the product salinity, ppm, will increase too. Increasing the product salinity is not favorable however, it will reduce the fresh water produced quality and their cost values too. Therefore, to obtain a suitable freshwater flow rates, m³/d, the feed salinity ratio (range X_f = 2–4 g/kg) found has no effect on the feed flow rate, on the other hand it is only necessary to operate the system at high powers to increase their productivity, m³/d (Fig. 14c). The feed salinity ratio will cause a reducing in feed flow rate and increase the product salinity. For instance, the percentage of reduce would become 83.34% at X_f = 2.500 g/kg (from 10 up

to 10 m³/d). However, the variation of these parameters will influence the SPC, kWh/m³ (Fig. 14d). Therefore, if it is manageable to increase the X_f, the SPC will become minimal.

The PV GA model is aimed to increase the power and the efficiencies. Therefore, the best operating conditions should be resulted from the PV GA model. The GA results are listed in Table 9. The results are indexed based on maximum module efficiency, maximum total power, maximum total efficiency, and electrical efficiency. For high module efficiency, the power output is recorded as a value of 1,538.19 W where the total efficiency is 8.114% and ambient temperature is about 33.46°C. Solar radiation should be 781 W/m², V_{oc} = 80.35 V, I_{pv} = 3.068 Å, and R = 1.5 ohm. For maximum power (=1,593 W), the module efficiency is equal to 4.3195%, the total efficiency = 8.59%, T_a = 31.9°C, I_s = 764 W/m², V_{oc} = 80.35 V, I_{pv} = 3.06 Å, and R = 1.5 ohm. Fig. 15 shows the percentage of the change between the indexed outputs based on the PV GA results. It is obviously clear that the change in the module efficiency is not significant enough. However, the optimum value is
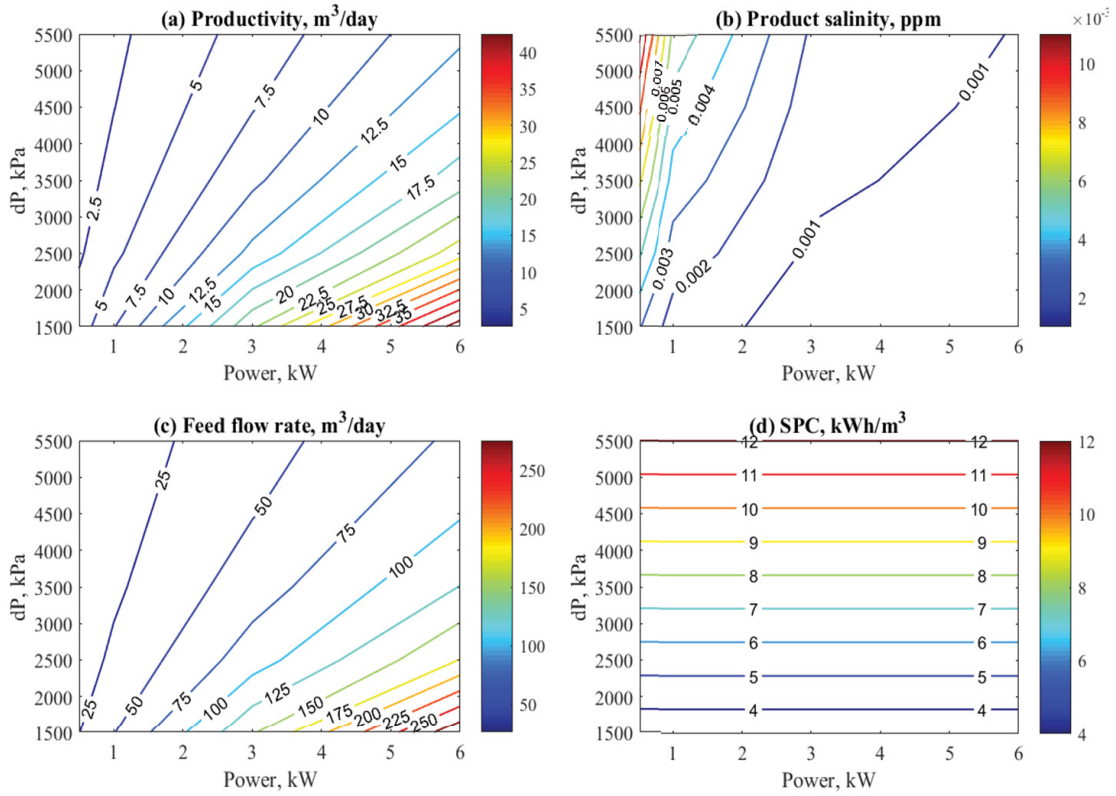
Fig. 13. Optimization results for proposed system based on the variation of power and pressure drop (RR = 15%; X_f = 2.5 g/kg): (a) productivity, m³/d, (b) product salinity, ppm, (c) feed flow rate, m³/d and (d) SPC, kWh/m³.
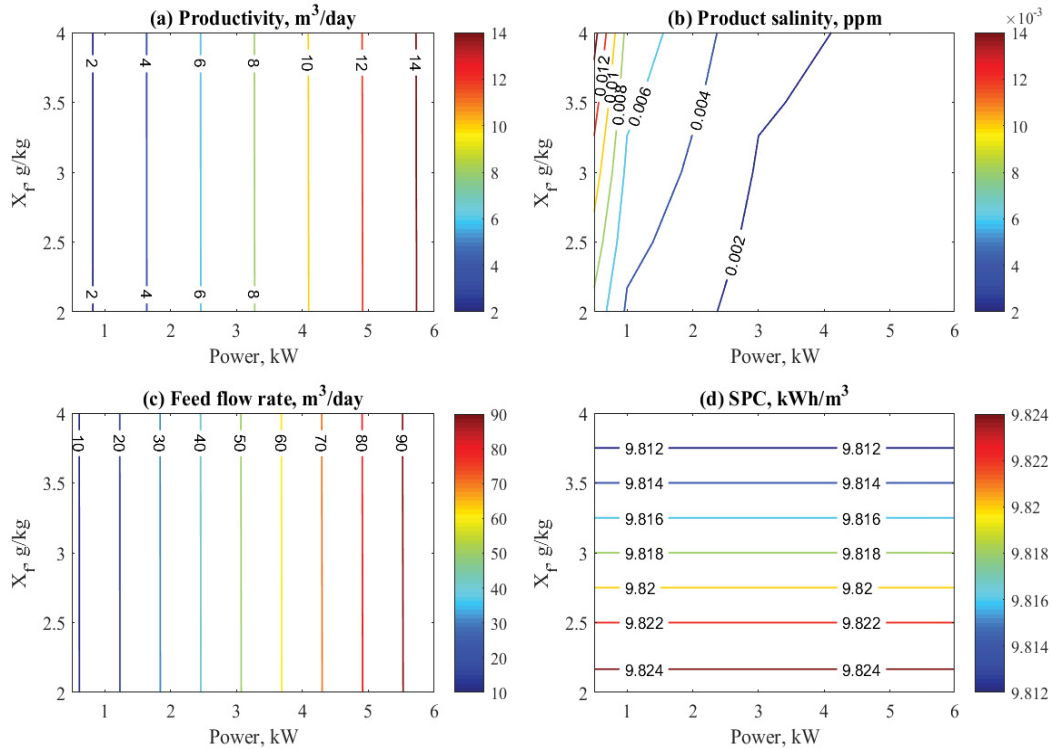

Fig. 14. Optimization results for proposed system based on the variation of power and feed salinity ratio (RR = 15%; d_p = 3,500 kPa): (a) productivity, m³/d, (b) product salinity, ppm, (c) feed flow rate, m³/d and (d) SPC, kWh/m³.
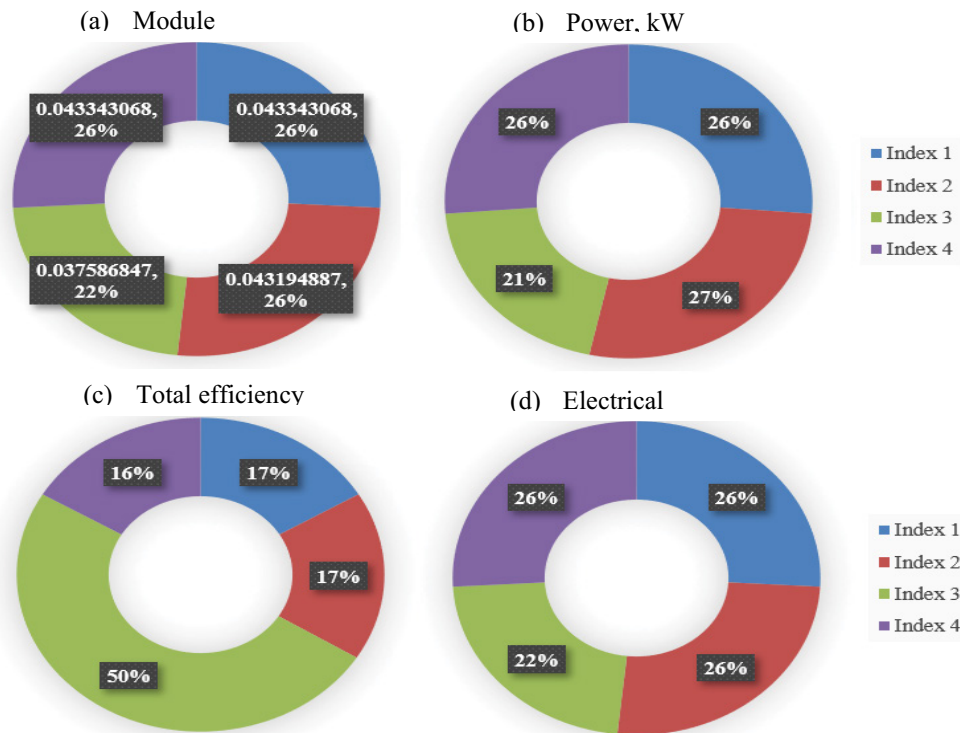
Fig. 15. Indexed results based on the PV/GA objective functions. (a) Module efficiency, (b) power, kW, (c) total efficiency and (d) electrical efficiency.
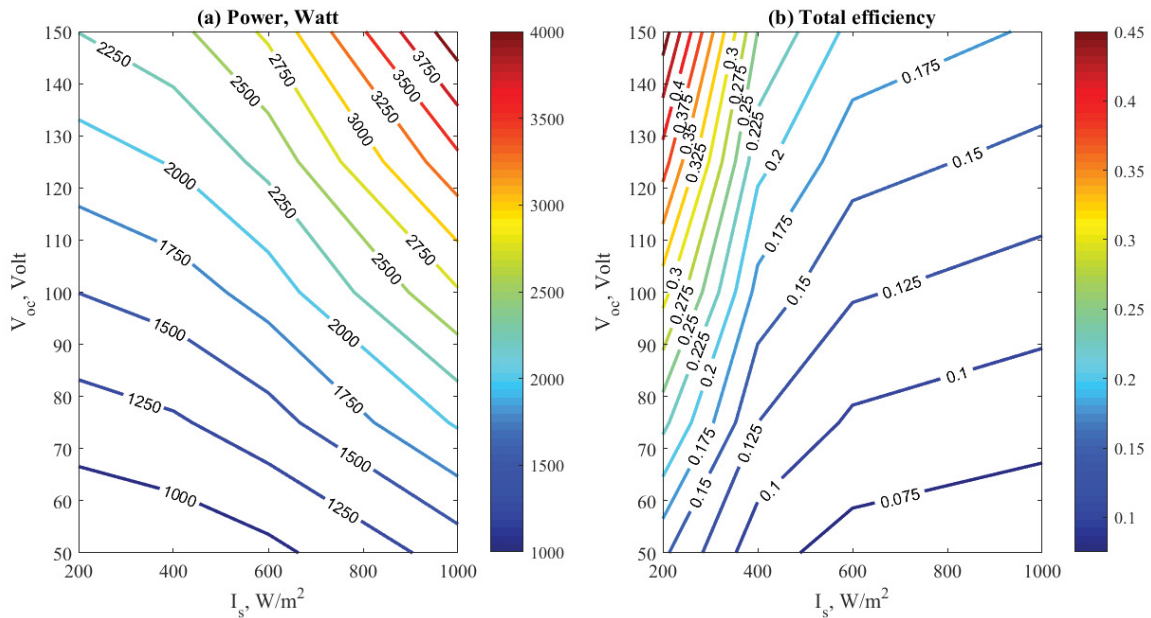

Fig. 16. The optimum variation of (a) power, Watt and (b) total efficiency based on the variations of solar radiation and open-circuit voltage.

centerlines around 4.3%. The significant change is occurred to the power while indexing to the total efficiency (Index 3). Where, the power from index 3 represents only 21% followed by the rest. High power is found under index 2 as anticipated. Generally, indexing with respect to the output

power should be claimed where the open-circuit voltage is about 80 V, and the solar radiation is about 764 W/m². Fig. 16 shows the optimum variations of output power and system total efficiency based on the variations of solar radiation and open-circuit voltage parameters. As shown

Table 9
GA index results for the PV system

Optimum output				Best individuals' variables				
η_m	Power, W	η_{tot}	η_{ele}	T_a, °C	I_s, W/m^2	V_{oc}, V	I_{pv}, Å	R, ohm
0.0433	1,538.198	0.0811	0.0487	33.464	781.110	80.352	3.069	1.501
0.0432	1,593.45	0.0859	0.0485	31.912	764.054	80.159	3.036	1.500
0.0422	1,334.703	0.1092	0.0474	30.761	503.725	80.212	3.011	1.501
0.0376	1,153.596	0.2367	0.0423	33.366	200.773	80.068	3.030	1.500
0.0376	1,189.788	0.2451	0.0422	30.063	200.000	80.000	3.000	1.500
0.0376	1,189.788	0.2451	0.0422	30.063	200.000	80.000	3.000	1.500
0.0432	**1,593.45**	0.0859	0.0485	31.912	764.054	80.159	3.036	1.500
0.0433	**1,538.198**	0.0811	0.0487	33.464	781.110	80.352	3.069	1.501
0.0422	**1,334.703**	0.1092	0.0474	30.761	503.725	80.212	3.011	1.501
0.0376	**1,189.788**	0.2451	0.0422	30.063	200.000	80.000	3.000	1.500
0.0376	**1,189.788**	0.2451	0.0422	30.063	200.000	80.000	3.000	1.500
0.0376	**1,153.596**	0.2367	0.0423	33.366	200.773	80.068	3.030	1.500
0.0376	1,189.788	**0.2451**	0.0422	30.063	200.000	80.000	3.000	1.500
0.0376	1,189.788	**0.2451**	0.0422	30.063	200.000	80.000	3.000	1.500
0.0376	1,153.596	**0.2367**	0.0423	33.366	200.773	80.068	3.030	1.500
0.0422	1,334.703	**0.1092**	0.0474	30.761	503.725	80.212	3.011	1.501
0.0432	1,593.45	**0.0859**	0.0485	31.912	764.054	80.159	3.036	1.500
0.0433	1,538.198	**0.0811**	0.0487	33.464	781.110	80.352	3.069	1.501
0.0433	1,538.198	0.0811	**0.0487**	33.464	781.110	80.352	3.069	1.501
0.0432	1,593.45	0.0859	**0.0485**	31.912	764.054	80.159	3.036	1.500
0.0422	1,334.703	0.1092	**0.0474**	30.761	503.725	80.212	3.011	1.501
0.0376	1,153.596	0.2367	**0.0423**	33.366	200.773	80.068	3.030	1.500
0.0376	1,189.788	0.2451	**0.0422**	30.063	200.000	80.000	3.000	1.500
0.0376	1,189.788	0.2451	**0.0422**	30.063	200.000	80.000	3.000	1.500

Note: The following parameters are considered constants for the PV GA model.
A_c = 0.024 m^2; KI = 0.0017 Å/°C; IF = 1.3; NOCs = 60; NOCp = 1; NOM = 15; BF = 0.89; FF = 0.88

in Fig. 16a, increasing the solar radiation would increase the power up to a certain limit. Besides that, increasing the V_{oc}, V would increase the power as expected. For instance, at 1,000 W/m^2 and 100 V, the generated power is about 1,500 W (1.5 kW). However, at 1,000 W/m^2 and 150 V, the power is recorded as 2,250 W (2.250 kW). For the total efficiency, maximum efficiency would occur at low values of the solar radiation and high values of the open-circuit voltage. For instance, at 200 W/m^2 and 130 V, the efficiency is recorded around 40%.

7. Conclusion

This developed work is concerning the combination and optimization between solar photovoltaic/battery and the reverse osmosis desalination process. The environmental conditions of operating system are put in mind the location of Casablanca, Morocco where the real system is established. It is aimed to desalinate brackish water source with a salinity ratio of 2–2.5 g/kg to produce about 1–5 m^3/d of freshwater. As it is well known, the combination is performed, however, it would be quite interested to optimize the system performance in order to reduce the SPC, kWh/m^3, that is, increase the system productivity. For that

purpose, GA model is performed and used in this work to optimize the system objective functions such as productivity, product salinity, SPC, PV efficiency, total power, and electric efficiency. The main target of the GA model is to decide the best operating condition that can lead to high rate of production, that is, low SPC. The recommended results can be withdrawn as following:

- A developed simulation model is performed to model and simulate the PV/battery/RO system. The model validation showed a remarkable matching with the real system.
- GA mathematical model is performed to enhance the system productivity via objective.
- Increasing the solar radiation will increase the total system productivity. The GA results show that a value of ~765 W/m^2 is quite remarkable to increase the productivity.
- A PV power values of 2–4 kW are optimum for the RO productivity under the feed flow temperature of 26°C. The SPC, kWh/m^3, is optimized from 12 down to 2.6 kWh/m^3.
- The optimum RO pressure is about 1,500 kPa with pumping efficiency of 80% and RR equal to 19% instead of 15%.

Symbols

A	—	Area, m²
BF	—	Backing factor, %
B_f	—	Packing factor, %
Bp	—	Battery power, W
BW	—	Brackish water
C_p	—	Specific heat capacity, kJ/kg°C at constant pressure
DOD	—	Battery depth of discharge
E_{go}	—	Band gap, eV
FF	—	Fill factor, %
GA	—	Genetic algorithm
GPV	—	Photovoltaic generator
H	—	Altitude, m
HHP	—	High-pressure pump, kW
I	—	Current, Å
IF	—	Ideality factor
I_s	—	Solar radiation, W/m²
KI	—	Short-circuit coefficient, Å/°C
L	—	Length, m, Latitude, °
l	—	Longitude, °
LF	—	Load factor, %
M	—	Mass flow rate, m³/h, kg/s
N,n	—	Number, #
NOC	—	Number of cloudy days
NOM	—	Number of modules, #
OH	—	Operating hours, h
P	—	Power, kW, or Pressure, bar
ppm	—	Parts per million
q	—	Electron charge, C
RO	—	Reverse osmosis
RR	—	Recovery ratio
R_s	—	Resistance, ohm
SPC	—	Specific power consumption, kWh/m³
SR	—	Salt rejection
STC	—	Standard test conditions: irradiation 1,000 W/m²; Cell temperature 25°C; AM 1.5
SW	—	Seawater
T	—	Temperature, °C
t	—	Time, h
TBP	—	Total battery bank power, kW
V	—	Voltage, V
Wco	—	Water costs, $/m³
X	—	Salinity ratio, g/kg (ppm)
Y	—	Extraction percentage, %

Subscripts

a	—	Ambient
av	—	Average
b	—	Brine
Batt,b	—	Battery
c	—	charge
d	—	Distillate product, discharge
e	—	Element
ec	—	Electrical
f	—	Feed
h	—	High
l	—	Load
m	—	Module
o	—	Saturation
oc	—	Open circuit
p	—	Product or pump, parallel
ph	—	photon
pv	—	Photovoltaic
s	—	Series
sc	—	Short circuit
scr	—	Reverse saturation
th	—	Thermal
total	—	Total
w	—	Water

Greek

Δ	—	Difference
η	—	Efficiency, %
ρ	—	Density, kg/m³
π	—	Osmotic pressure, kPa

References

[1] N. Misdan, W.J. Lau, A.F. Ismail, Seawater reverse osmosis (SWRO) desalination by thin-film composite membrane—current development, challenges and future prospects, Desalination, 287 (2011) 228–237.

[2] A. Lilane, D. Saifaoui, S. Hariss, H. Jenkal, M. Chouiekh, Modeling and simulation of the performances of the reverse osmosis membrane, Mater. Today Proc., 24 (2019) 114–118.

[3] W. Khiari, M. Turki, J. Belhadj, Robust DC-bus voltage control for batteryless brackish water reverse osmosis desalination prototype operating with variable wind and solar irradiation, Int. J. Renewable Energy Res., 8 (2017) 1544–1552.

[4] R. Danoun, Desalination Plants: Potential Impacts of Brine Discharge on Marine Life, The Ocean Technology Group, The University of Sydney, Australia, 2007.

[5] A. Lilane, D. Saifaoui, Y. Aroussy, S. Hariss, M. Oulhazzan, Experimental study of a pilot membrane desalination system: the effects of transmembrane pressure, Mater. Today Proc., 30 (2020) 970–975.

[6] B.D. Negewo, Ed., Renewable Energy Desalination: An Emerging Solution to Close the Water Gap in the Middle East and North Africa, World Bank Publications, 2012.

[7] A. Al-Karaghouli, L.L. Kazmerski, Energy consumption and water production cost of conventional and renewable-energy-powered desalination processes, Renewable Sustainable Energy Rev., 24 (2012) 343–356.

[8] M.A. Dawoud, M.M. Al Mulla, Environmental impacts of seawater desalination: Arabian Gulf case study, Int. J. Environ. Sustainability, 1 (2012) 22–37.

[9] S.A. Avlonitis, K. Kouroumbas, N. Vlachakis, Energy consumption and membrane replacement cost for seawater RO desalination plants, Desalination, 157 (2003) 151–158.

[10] T.M. Missimer, N. Ghaffour, A.H. Dehwah, R. Rachman, R.G. Maliva, G. Amy, Subsurface intakes for seawater reverse osmosis facilities: capacity limitation, water quality improvement, and economics, Desalination, 322 (2013) 37–51.

[11] P.S. Bhambare, M.C. Majumder, C.V. Sudhir, Solar thermal desalination: a sustainable alternative for sultanate of Oman, Int. J. Renewable Energy Res., 8 (2018) 733–751.

[12] J.S. Kim, J. Chen, H.E. Garcia, Modeling, control, and dynamic performance analysis of a reverse osmosis desalination plant integrated within hybrid energy systems, Energy, 112 (2016) 52–66.

[13] K. Quteishat, Abu-Arabi, Promotion of Solar Desalination in the MENA Region, Middle East Desalination Res. Cent., Muscat, Oman, 2012.

[14] N. Kannan, D. Vakeesan, Solar energy for future world – a review, Renewable Sustainable Energy Rev., 62 (2016) 1092–1105.

[15] Solar Resource Data: Solargis © 2019 The World Bank, Source: Global Solar Atlas 2.0. Available at: https://solargis.com/maps-and-gis-data/download/world, consulted 31/05/2020

[16] M. Qadir, B.R. Sharma, A. Bruggeman, R. Choukr-Allah, F. Karajeh, Non-conventional water resources and opportunities for water augmentation to achieve food security in water scarce countries, Agric. Water Manage., 87 (2007) 2–22.

[17] R. Ragab, A. Hamdy, Water Management Strategies to Combat Drought in the Semiarid Regions, Water Manag. Drought Mitig. Mediterr. Cent. Int. Hautes Etudes Agron. Méditerranéennes Tecnomack–Bari Italy, 2004, pp. 47–112.

[18] Z. Al Suleimani, V.R. Nair, Desalination by solar-powered reverse osmosis in a remote area of the Sultanate of Oman, Appl. Energy, 65 (2000) 367–380.

[19] D. Herold, A. Neskakis, A small PV-driven reverse osmosis desalination plant on the island of Gran Canaria, Desalination, 137 (2001) 285–292.

[20] M. Thomson, D. Infield, A photovoltaic-powered seawater reverse-osmosis system without batteries, Desalination, 153 (2003) 1–8.

[21] I. de la Nuez Pestana, F.J.G. Latorre, C.A. Espinoza, A.G. Gotor, Optimization of RO desalination systems powered by renewable energies. Part I: wind energy, Desalination, 160 (2004) 293–299.

[22] E.S. Mohamed, G. Papadakis, Design, simulation and economic analysis of a stand-alone reverse osmosis desalination unit powered by wind turbines and photovoltaics, Desalination, 164 (2004) 87–97.

[23] E.S. Mohamed, G. Papadakis, E. Mathioulakis, V. Belessiotis, A direct coupled photovoltaic seawater reverse osmosis desalination system toward battery based systems—a technical and economical experimental comparative study, Desalination, 221 (2008) 17–22.

[24] M. Monnot, G.D.M. Carvajal, S. Laborie, C. Cabassud, R. Lebrun, Integrated approach in eco-design strategy for small RO desalination plants powered by photovoltaic energy, Desalination, 435 (2018) 246–258.

[25] I.D. Spyrou, J.S. Anagnostopoulos, Design study of a stand-alone desalination system powered by renewable energy sources and a pumped storage unit, Desalination, 257 (2010) 137–149.

[26] A. Al-Karaghouli, L. Kazmerski, Economic and technical analysis of a reverse-osmosis water desalination plant using DEEP-3.2 software, J. Environ. Sci. Eng. A, 1 (2012) 318–328.

[27] E.M. Mokheimer, A.Z. Sahin, A. Al-Sharafi, A.I. Ali, Modeling and optimization of hybrid wind–solar-powered reverse osmosis water desalination system in Saudi Arabia, Energy Convers. Manage., 75 (2013) 86–97.

[28] T. Ben M'Barek, K. Bourouni, K.B. Ben Mohamed, Optimization coupling RO desalination unit to renewable energy by genetic algorithms, Desal. Water Treat., 51 (2013) 1416–1428.

[29] A. Alsheghri, S.A. Sharief, S. Rabbani, N.Z. Aitzhan, Design and cost analysis of a solar photovoltaic powered reverse osmosis plant for Masdar Institute, Energy Procedia, 75 (2015) 319–324.

[30] I.J. Esfahani, C. Yoo, An optimization algorithm-based pinch analysis and GA for an off-grid batteryless photovoltaic-powered reverse osmosis desalination system, Renewable Energy, 91 (2016) 233–248.

[31] M.A. Alghoul, P. Poovanaesvaran, M.H. Mohammed, A.M. Fadhil, A.F. Muftah, M.M. Alkilani, K. Sopian, Design and experimental performance of brackish water reverse osmosis desalination unit powered by 2 kW photovoltaic system, Renewable Energy, 93 (2016) 101–114.

[32] J. Shen, B.S. Richards, A.I. Schäfer, Renewable energy powered membrane technology: case study of St. Dorcas borehole in Tanzania demonstrating fluoride removal via nanofiltration/reverse osmosis, Sep. Purif. Technol., 170 (2016) 445–452.

[33] G. Zhang, B. Wu, A. Maleki, W. Zhang, Simulated annealing-chaotic search algorithm based optimization of reverse osmosis hybrid desalination system driven by wind and solar energies, Sol. Energy, 173 (2018) 964–975.

[34] O. Charrouf, A. Betka, S. Abdeddaim, A. Ghamri, Artificial neural network power manager for hybrid PV-wind desalination system, Math. Comput. Simul., 167 (2020) 443–460.

[35] G.D.P. da Silva, M.H. Sharqawy, Techno-economic analysis of low impact solar brackish water desalination system in the Brazilian Semiarid region, J. Cleaner Prod., 248 (2020) 119255, doi: 10.1016/j.jclepro.2019.119255.

[36] T.A. Ajiwiguna, G.-R. Lee, B.-J. Lim, S.-H. Cho, C.-D. Park, Optimization of battery-less PV-RO system with seasonal water storage tank, Desalination, 503 (2021) 114934, doi: 10.1016/j.desal.2021.114934.

[37] E. Rosales-Asensio, A.-E. Rosales, A. Colmenar-Santos, Surrogate optimization of coupled energy sources in a desalination microgrid based on solar PV and wind energy, Desalination, 500 (2021) 114882, doi: 10.1016/j.desal.2020.114882.

[38] S. Saravanan, S. Thangavel, A simple power management scheme with enhanced stability for a solar PV/wind/fuel cell/grid fed hybrid power supply designed for industrial loads, J. Electr. Comput. Eng., 2014 (2014) 319017, doi: 10.1155/2014/319017.

[39] K.L. Lian, J.H. Jhang, I.S. Tian, A maximum power point tracking method based on perturb-and-observe combined with particle swarm optimization, IEEE J. Photovoltaics, 4 (2014) 626–633.

[40] M.E. Ropp, S. Gonzalez, Development of a MATLAB/simulink model of a single-phase grid-connected photovoltaic system, IEEE Trans. Energy Convers., 24 (2009)195–202.

[41] D. Rekioua, E. Matagne, Optimization of Photovoltaic Power Systems: Modelization, Simulation and Control, Green Energy and Technology, Springer, 2012.

[42] V. Azbe, R. Mihalic, Distributed generation from renewable sources in an isolated DC network, Renewable Energy, 31 (2006) 2370–2384.

[43] R. Burgos, D. Boroyevich, F. Wang, K. Karimi, G. Francis, On the AC Stability of High Power Factor Three-Phase Rectifiers, Proc. Energy Convers. Congr. Expo., 2010, pp. 2047–2054.

[44] G.N. Tiwari, S. Dubey, Fundamentals of Photovoltaic Modules and Their Applications, RSC Publishing, 2010.

[45] M.A. Sharaf Eldean, A. El Shahat, A.M. Soliman, A new modeling technique based on performance data for photovoltaic modules and horizontal axis wind turbines, Wind Eng., 42 (2018) 209–229.

[46] G. Amy, N. Ghaffour, Z. Li, L. Francis, R.V. Linares, T. Missimer, S. Lattemann, Membrane-based seawater desalination: present and future prospects, Desalination, 401 (2017) 16–21.

[47] A. Roy, S. Moulik, R. Kamesh, A. Mullick, Eds., Modeling in Membranes and Membrane-based Processes, John Wiley & Sons Publications, New Jersey, 2020.

[48] A.S. Nafey, M.A. Sharaf, L. García-Rodríguez, Thermo-economic analysis of a combined solar organic Rankine cycle-reverse osmosis desalination process with different energy recovery configurations, Desalination, 261 (2010) 138–147.

[49] A.S. Nafey, M.A. Sharaf, Combined solar organic Rankine cycle with reverse osmosis desalination process: energy, exergy, and cost evaluations, Renewable Energy, 35 (2010) 2571–2580.

[50] A.M. Soliman, A. Mabrouk, M.A.S. Eldean, H.E. Fath, Techno-economic analysis of the impact of working fluids on the concentrated solar power combined with multi-effect distillation (CSP-MED), Desal. Water Treat., 210 (2021) 1–21.

[51] D. Rani, S.K. Jain, D.K. Srivastava, M. Perumal, Genetic algorithms and their applications to water resources systems, Metaheuristics Water Geotech. Transp. Eng., 43 (2013), doi: 10.1016/B978-0-12-398296-4.00003-9.